POLITECNICO DI TORINO

Corso di Laurea Magistrale

in Renewable Energy Systems

Tesi di Laurea Magistrale

Adsorbent Materials for Biomethane Applications to be used in a Cogeneration Plant to produce Electricity and Home Heating

Relatori

Prof.ssa Debora Fino

Prof.ssa Francesca Demichelis

Candidato

Maragjulia Vuksani

Summary

Introduction

1.1 Thesis Objective

The objective of this thesis is to evaluate and implement experimental tests for the removal of acidic compounds from a process stream, within the framework of a research project developed in collaboration with HYSYTECH S.r.l. The core focus of this study is the application and optimization of Micro-Bio-CHP technology, which is part of an initiative funded by the EU Horizon 2020 program.

The primary issue addressed by this thesis revolves around the decarbonization of the residential energy sector, particularly the excessive reliance on fossil fuels for domestic heating and electricity production. In the current context, micro-CHP technologies based on conventional combustion or Stirling engines fail to meet household energy demands due to both low electrical efficiency and significant environmental impact.

The innovative aspect of Micro-Bio-CHP lies in integrating a gasifier with a Solid Oxide Fuel Cell (SOFC), enabling the simultaneous production of heat and electricity from renewable sources, specifically biomass. This approach achieves:

- Electrical efficiency of 44% related to the calorific value of the produced gas.
- A significant reduction in CO, organic gaseous compounds (OGC), particulate matter, and NOx emissions compared to conventional biomass-based CHP technologies.
- A combination with photovoltaic (PV) systems to ensure continuous renewable energy supply throughout the year, overcoming the seasonal limitations of biomass micro-CHP systems.

The original contribution of this thesis lies in the development of a MATLAB code to model the system's behavior and in updating the engineering documentation of the project: these tools allow for simulating system performance, optimizing the test bench configuration to ensure maximum efficiency year-round, even during periods of low heat demand.

This thesis outlines the work carried out at HYSYTECH S.r.l. starting from March 2024. The objective of this study is the application of experimental tests aimed at the removal of acidic compounds from a process stream.

Initially, the project to which this thesis belongs will be presented, describing its goals and current state of the art. This will be followed by an analysis of the chemical-physical principles underlying the modelling calculations, before focusing in detail on the work conducted.

Specifically, the functioning of the test bench was conceptualized, in which all the equipment and piping had already been sized by the previous thesis student last year, who has now assumed the role of my supervisor. Subsequently, a MATLAB code capable of modelling the system's behaviour was developed, and the detailed engineering documents were updated.

1.2 Host company

This thesis is part of a research project carried out in collaboration with HYSYTECH S.r.l., a company known for its specialization in developing and implementing innovative industrial processes. With its active participation in numerous research initiatives, HYSYTECH demonstrates a strong commitment to driving innovation in sustainable technologies. One of these initiatives, the Micro-Bio-CHP project, is the subject of this thesis, reflecting HYSYTECH’s leading role in Italy’s sustainable technology landscape.

The company focuses on areas like renewable energy recovery, energy production, and industrial gas treatment, with a strong commitment to solutions that promote both sustainability and a circular economy.

It was partially acquired by Nippon Gases, further enhancing the company’s ability to advance cutting-edge energy technologies.

The Project

2.1 Micro-Bio-CHP

The MBC project, launched on October 1st, 2022, is part of the EU Horizon 2020 framework, which funds research initiatives with a focus on scientific and technological advancements that can greatly benefit European citizens. MBC leverages cutting-edge developments in micro-scale cogeneration systems, designed to deliver both heat and electricity to homes. The project's key goal is to significantly reduce carbon emissions in the domestic energy sector by introducing a novel approach to combined heat and power generation technology.

Figure 1. MBC Project logo

As highlighted on the Hysytech website, MBC integrates a gasifier with a Solid Oxide Fuel Cell (SOFC) to produce heat and electricity simultaneously for residential use. This innovative solution offers a highly efficient and cost-effective energy generation system.

2.2 Main scopes

In 2021, household energy consumption represented around 28% of the EU's final energy use, contributing to 17% of the total inland energy demand (Eurostat). Of this, the majority—63.6%—was used for space heating, followed by 14.8% for domestic hot water, 14.1% for lighting and appliances, and 6.1% for cooking. This places household energy consumption second only to the transport sector (29%), and ahead of industry (25%).

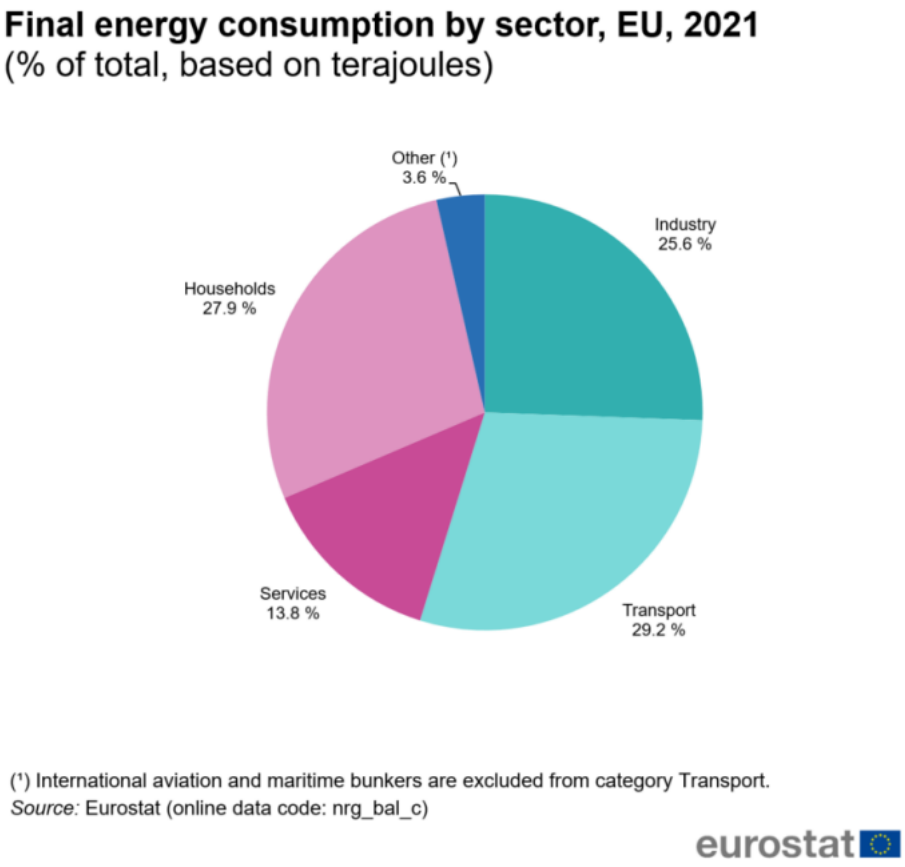

Figure 2. Final energy consumption by sector (source: Eurostat)

For space heating, renewable sources accounted for just 27.9%, while fossil fuels still dominated with 42%, alongside derived heat (10.1%) and electricity (5.3%). For domestic hot water, natural gas led with 40.9%, while renewables and electricity contributed 13.1% and 20.2%, respectively. In cooking, electricity was the main energy source (49.8%), followed by natural gas (31%) and oil (13%). Despite these numbers, natural gas remains the leading household energy source overall, followed by electricity (24.7%) and renewables (19.5%).

Achieving deep decarbonization in the EU's residential sector will require a significant shift from fossil fuels to renewable energy systems, particularly as 38% of the EU's electricity production in 2021 was still reliant on fossil sources (Eurostat). One critical solution to this challenge is the adoption of micro-scale combined heat and power (CHP) systems powered by renewable energy. According to EU Directive 2012/27/EU, these CHP units—limited to under 50 kW electrical capacity—are vital, particularly for single and multi-family homes, where even smaller units (<10 kW) are necessary.

Current technologies such as Stirling engines provide limited electric output (around 600 W) and low efficiency (under 10%). Other options, like steam engines and Organic Rankine Cycles (ORCs), are still under research and development, while thermoelectric generators available today have low capacities (<0.25 kW) and minimal efficiencies (1.3% to 2.5%), making them unsuitable for household energy demands.

To progress, more efficient and reliable biomass-based micro-CHP systems are needed. These systems not only need to improve electrical efficiency but also address the pressing need to

reduce gaseous and particulate emissions, aligning with the European Green Deal's zero-pollution goal. One promising strategy is combining biomass micro-CHP systems with photovoltaic (PV) technologies. This hybrid solution ensures a continuous supply of renewable energy throughout the year, particularly during summer, when heat demand is low and traditional biomass CHP systems would otherwise be inefficient.

The Micro-Bio-CHP project aims to tackle these challenges head-on by developing a renewable energy-based system for residential heat and electricity supply. The goal is near-energy autonomy for multi-family buildings, covering space heating, domestic hot water, electricity needs, and even contributing to electric mobility. This innovative approach involves integrating a biomass micro-CHP system—featuring an updraft gasifier, advanced gas cleaning technology, and a solid oxide fuel cell (SOFC)—with a high-efficiency PV system. The result is a low-emission, high-performance energy solution capable of meeting all household energy needs.

By incorporating this advanced CHP technology, the project expects to virtually eliminate CO, organic gaseous compounds (OGC), and particulate emissions, while achieving a 55% to 65% reduction in NOx emissions compared to conventional biomass CHP systems. The system also addresses the fluctuating heat, and electricity demands throughout the year. Biomass CHP systems, for instance, often struggle to operate continuously due to seasonal variations, only running at full capacity for about seven months of the year. Moreover, technologies like Stirling engines remain economically unfeasible due to their low electrical efficiency during transition seasons.

To overcome these issues, this project seeks to maximize electric efficiency by utilizing pellet gasification combined with an SOFC. This solution ensures high load hours for electricity production, making it highly reliable year-round.

From May to September, when heat demand is minimal, conventional CHP systems become inefficient. However, the opposite is true for PV systems, which produce the most electricity during this period. This makes the combination of biomass CHP and PV an ideal solution to provide renewable energy throughout the year. Not only can this system supply the building’s energy needs, but any surplus electricity can be diverted to charge electric vehicles, further enhancing energy sustainability for the occupants.

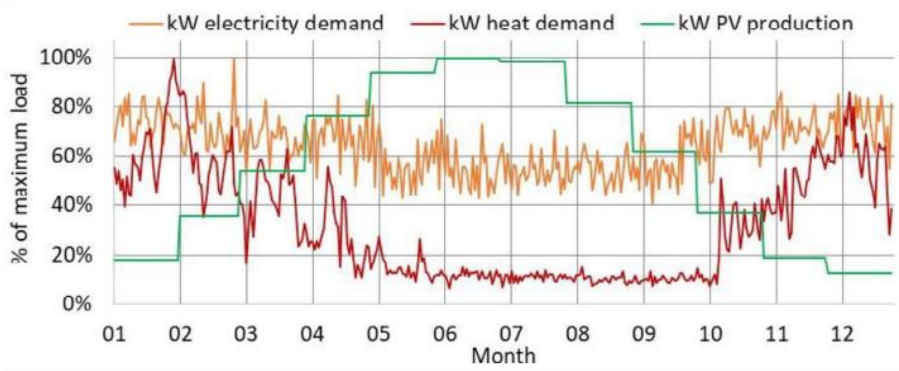

Figure 3. Heat and electricity demand of a typical multi-family house as well as PV electricity production over one year

2.2.1 The new innovative micro-bio-CHP technology

The Micro-Bio-CHP process introduces a breakthrough in small-scale biomass CHP systems. Unlike conventional setups, where all the energy from fuel conversion is directed toward electricity production, this innovative method takes a more strategic approach. A portion of the product gas is extracted from above the fuel bed and, after a thorough gas cleaning process, is sent to a Solid Oxide Fuel Cell (SOFC) for highly efficient electricity production—achieving an impressive 44% electrical efficiency based on the Net Calorific Value of the gas. Meanwhile, the remaining product gas is burned in a gas burner, with the resulting flue gases and SOFC off-gases directed to a heat recovery unit. This unit, which includes a boiler and a flue gas condenser, efficiently generates heat for the building.

The extracted product gas flow to the SOFC is carefully controlled to maintain continuous, high-load operation, ensuring maximum electricity generation even during periods of fluctuating heat demand, such as during the transition between seasons. When winter arrives and heat demand increases, the fuel power is ramped up, keeping the product gas flow to the SOFC within its optimal range. Simultaneously, more gas is routed through the burner to meet the rising heat needs. This dual-function system—combining base-load electricity production with flexible heat generation—creates a highly efficient and reliable energy supply for the building, even during peak load phases. This approach mirrors large district heating CHP plants, where two separate boilers are often required, but here it is compactly integrated into a single system.

The result is a pioneering biomass micro-CHP concept that maximizes the system's operation hours, making electricity generation more consistent and economically feasible. This innovative solution also incorporates a state-of-the-art photovoltaic (PV) system, which complements the CHP plant by gradually taking over electricity production during transitional seasons and fully during the summer months. During this time, when heat demand is low, the CHP plant goes offline, and domestic hot water (DHW) needs are met using a power-to-heat device powered by electricity from the PV system.

To address the wide fluctuations in daily heat and electricity demands, as well as variations in PV electricity production, the system is equipped with innovative energy storage solutions. For heat storage, a properly sized buffer tank with an integrated power-to-heat device ensures efficient energy use. On the electrical side, an intelligent control system ensures that any excess electricity is used to charge electric vehicles, while bi-directional charging technology (anticipated on the market by 2022–2023) allows stored energy in the vehicle batteries to be used for building supply during high-demand periods. This approach is expected to be highly efficient, particularly between February and October, when electricity production often exceeds the building's energy needs.

Another key feature of this system is its resilience. The partial product gas extraction setup allows the system to operate in heat-only mode—bypassing the SOFC—should any failure occur in the SOFC unit. In this scenario, the gasifier and burner continue to supply heat to the building, while the PV system can handle the majority, if not all, of the electricity demand, depending on the availability of solar energy. This design significantly enhances energy security, offering a more reliable solution compared to other biomass and solar energy systems.

To ensure ease of transport and installation, the system is divided into two modules: the biomass conversion module and the SOFC module. This modular approach simplifies logistics and allows for smoother integration into various building setups.

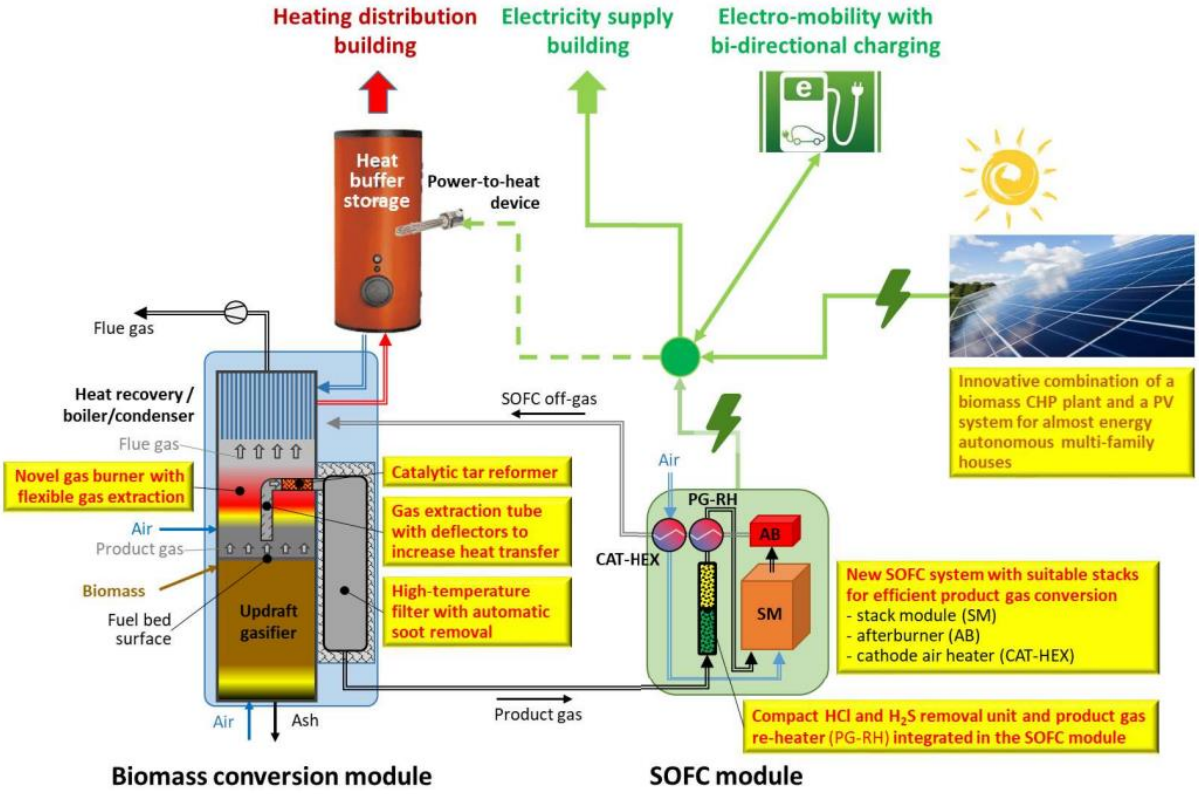

Figure 4. Scheme of the new concept for an almost energy autonomous and renewable energy based multi-family house

2.2.2 Detailed objectives

The project is based on typical heat and electricity demand profiles over a year for a multi-family house (9 apartments, 19 occupants) in the alpine region, meeting the ambitious Austrian standards for new low-energy buildings with a specific heating demand of 42 kWh/m2/year.

The project involves several key objectives for the development of the innovative biomass micro-CHP system:

- Development of a biomass updraft gasifier with a capacity range of 10-15 kW, operated with air and internally produced steam. The gasifier will be coupled with a novel product gas burner, fully oxidizing a portion of the product gas at near-zero CO, OGC, and PM emissions at full and minimum load. This burner also supplies energy for heating up the extracted product gas for electricity production in the SOFC.

- Design of a product gas extraction pipe with flow deflectors to enhance heat transfer and allow flexible control over the share of the extracted product gas, ranging between zero (heat-only operation) and about 50% at minimum thermal load operation.

- Development of a tar reforming catalyst based on precious metals (e.g., Pt, Rh) for application in the product gas extraction pipe at temperatures exceeding 900°C, aiming for tar conversion efficiencies above 90%.

- Creation of a hot gas filter for particle removal to levels below 1 mg/Nm3, downstream the product gas extraction tube, with a periodically applied back-burning system to remove soot deposits. This filter must operate at high temperatures and varying conditions, representing a key innovation.

- Design of a heat recovery system integrated into the biomass conversion module, consisting of a water jacket around the gasifier and product gas burner, steam generators, a heat exchanger, and a condenser to achieve an overall plant efficiency of over 90%.

- Development and design of a compact and easily maintainable sorption reactor for HCl and H2S removal with target values of <5 ppm HCl and <1 ppm H2S at SOFC inlet.

- Further development and optimization of SOFC stacks for operation with product gas from biomass updraft gasification, focusing on process control, stack degradation, homogeneous gas flow, enhanced lifetime, and high fuel utilization and electric efficiencies on stack level.

- Integration of the SOFC system, including the stack unit, cathode air pre-heater, catalytic afterburner, and process control, with the sorption reactor and a product gas re-heater into a compact single unit—the SOFC module.

- Development of an overall process control system for the biomass micro-CHP system.

- Construction of a testing plant for the CHP system, integrating it into the existing testing facilities at BIOS, including a buffer storage, PV system, and car battery charging stations for comprehensive testing of the entire concept.

2.2.3 Work program and R&I maturity

The project's work plan is structured into work packages (WPs) aimed at achieving the objectives outlined earlier.

1. **Project Management**
    - This WP is dedicated to overseeing the project's administration, ensuring smooth progress, and managing communication between partners.
2. **System Design**
    - The initial phase focuses on defining the system design. This includes specifying the components of the biomass conversion module and the Solid Oxide Fuel Cell (SOFC) module, particularly addressing the integration of H2S and HCl removal processes.
3. **Biomass Conversion Module Development**
    - These WPs handle the research and innovation (R&I) activities related to the development of the biomass conversion module. This involves optimizing gas reforming and gas filtration processes.
4. **SOFC Module Development**
    - WP5 focuses on the development of the SOFC module, including detailed work on the removal of harmful compounds such as H2S and HCl to ensure the efficient and safe operation of the fuel cells.
5. **Testing Plant Construction**
    - A testing plant representing the entire Combined Heat and Power (CHP) system will be designed and constructed. This plant will be used for extensive testing and optimization of the system components.
6. **Testing and Optimization**
    - This WP is divided into three testing phases. Each phase involves testing the system, evaluating results, identifying weaknesses, and implementing improvements. Feedback loops are established to ensure continuous enhancement of both individual components and the overall system.
7. **Techno-Economic and Environmental Assessments**
    - It performs techno-economic analyses, environmental impact assessments, and disseminates the project results. This WP is crucial for evaluating the economic viability and environmental benefits of the new technology.

The project aligns with the objectives of the funding call, aiming to develop a highly efficient and virtually zero-emission energy system. This system combines bioenergy and solar energy, ensuring a CO_2-neutral energy supply for residential buildings. The project emphasizes:

- Integration of bioenergy and solar energy: the system aims to provide not only the energy required by residential buildings but also electricity for electro-mobility, supporting a CO_2-neutral footprint.
- Emission reductions: by developing an ultra-low emission product gas burner and integrating catalytic afterburners, the system aims to achieve near-zero emissions of CO, organic gaseous compounds (OGC), and particulate matter (PM), along with significantly reduced NOx emissions.
- Technology readiness: the project's core technology, the novel biomass CHP plant, requires comprehensive R&I activities. While some components like PV modules and power-to-heat devices are already state-of-the-art, the biomass CHP plant itself demands significant innovation and development.

The R&I activities will leverage existing technologies and expertise, such as:

- Fixed-Bed Updraft Gasifier Technology: This technology is already market-proven and will serve as a foundation for developing the new biomass CHP system.
- Heat Recovery and Gas Cleaning: Established heat recovery technologies and knowledge of gas cleaning and SOFC systems will be crucial in the development process.

The project will focus on several key innovations to achieve its goals:

- Ultra-Low Emission Product Gas Burner: Developing a burner technology suitable for a broad power range, ensuring ultra-low emissions from the biomass gasification process.
- Flexible Product Gas Extraction: Creating a new concept for extracting and heating product gas for electricity production in the SOFC, following gas cleaning.
- Combined Thermal and Catalytic Tar Reforming: Innovating tar reforming processes to improve the efficiency and cleanliness of the product gas.
- High-Temperature Filter with Soot Removal: Developing a novel filter that effectively removes soot and other particulates from the gas stream.
- SOFC Stacks and Process Control: Tailoring SOFC stacks and control processes to handle cleaned product gases from biomass gasification, ensuring high efficiency and low degradation.
- Compact SOFC Module: Integrating HCl and H2S removal within a compact SOFC module, along with the stack unit and other necessary components, to minimize space and maximize efficiency.

The proposed project aims to develop a highly efficient micro-scale combined heat and power (CHP) system based on pellet gasification and a solid oxide fuel cell (SOFC). This system

seeks to maximize electric efficiency and operational hours, particularly during transitional seasons, ensuring continuous high-load SOFC operation and maximizing electricity production from biomass.

Gasifier and SOFC Development

The fixed-bed updraft gasifier technology is scaled down to a capacity range of about 10-15 kW fuel power. Wood pellets are chosen as the biomass fuel due to their advantageous transport and storage properties. The gasifier will be operated with air and steam, with steam addition controlling the temperatures in the charcoal burnout zone. The product gas produced will be used for heat production in the product gas burner and the subsequent heat recovery unit (boiler), as well as for SOFC operation.

Gas Cleaning and Tar Reforming

The project leverages extensive know-how and experience in removing particulate matter (PM), sulfur (S), and chlorine (Cl) from biomass gasifiers, as well as thermal and catalytic reforming of tars. The combined thermal and catalytic tar reforming with efficiencies greater than 99.9% is a novel approach. The cleaned product gas is essential for the long-term, highly efficient operation of the SOFC. The develop of SOFC stacks and process controls tailored to the characteristics of cleaned product gases from biomass updraft gasification are needed, aiming for highly efficient product gas conversion into electricity with low stack degradation rates and high stack lifetimes.

Testing and Validation

The technology's validation involves comprehensive test runs at a testing plant, aiming to achieve a Technology Readiness Level (TRL) of 5 by the project's end. The test runs will provide data to gradually update the mass and energy balancing tool and improve the final system design.

2.2.4 Framework Conditions and Application

The project considers the heat and electricity demand trends of residential buildings to ensure the technology is applicable for various building sizes and standards, including single-family and multi-family houses. Simulations will analyse real-life heat and electricity demand trends under different conditions, providing data for system design and operation scenarios. The overall process control concept will be developed based on a heat-controlled operation of the biomass CHP plant, integrating buffer storage and PV systems autonomously to facilitate various combinations with other manufacturers.

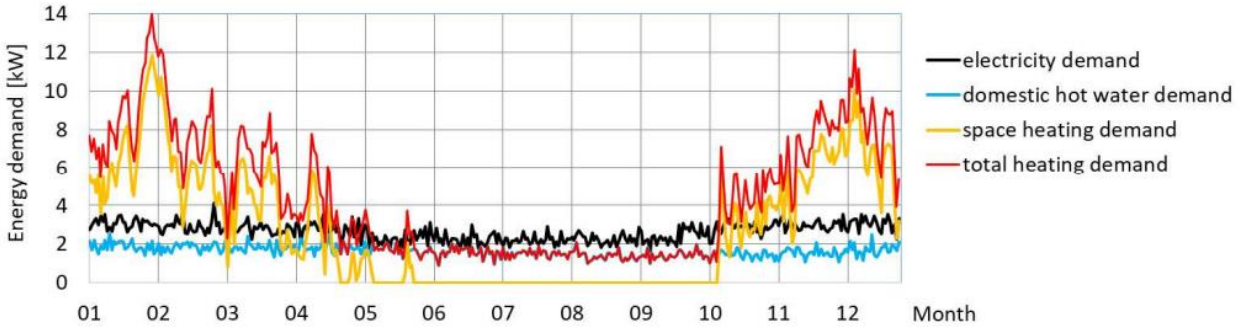

Figure 5. Annual heat and electricity demand profiles of a multi-family house with 9 apartments

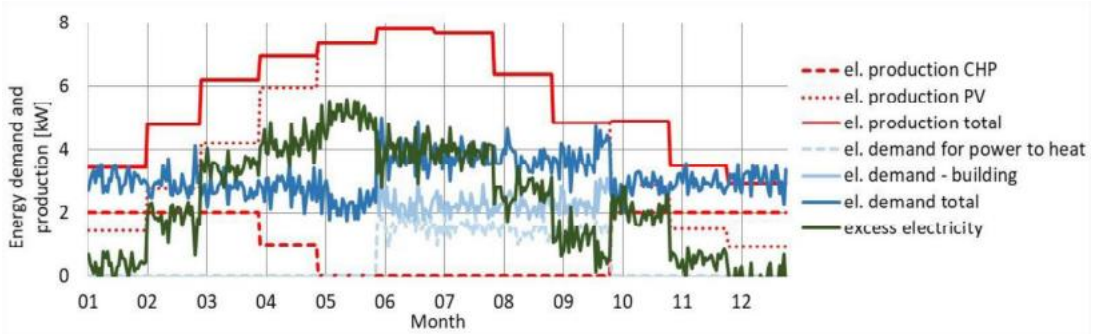

Figure 6. Targeted electricity production and consumption over the year

Simulation of the Project on AspenPlus Environment

The goal of this study is to evaluate the potential power production, including gross and net electrical output and thermal output, based on the inlet biogas flow available to the Solid Oxide Fuel Cell (SOFC) module parameters.

Reforming

Methane reformers, including steam reforming, autothermal reforming, and partial oxidation, are devices used in chemical synthesis to produce pure hydrogen gas from methane using a catalyst. Among the various reformers under development, autothermal reforming (ATR) and steam methane reforming (SMR) are the most commonly employed in the industry. These methods typically involve exposing methane to a catalyst, usually nickel, under high temperature and pressure conditions.

Steam reforming involves converting methane into hydrogen using steam, according to the following reaction:

$$CH_4 + H_2O \rightarrow CO + 3H_2$$

To prevent carbon deposition within the reactor, it is crucial to maintain an appropriate Steam to Carbon ratio (H_2O/CH_4). The reformer feed must contain sufficient steam to avoid thermal cracking of hydrocarbons and coke formation. Typically, an excess of steam beyond the stoichiometric ratio is used. Increasing the steam to carbon ratio reduces the residual methane for a given reformer outlet temperature, thus requiring less fuel energy in the furnace. Since the steam reforming reaction is endothermic, it necessitates an external heat source.

The reformer reactor can be:

External Reformer

- Heat is supplied by an external source, such as heat recovery from the system or a dedicated natural gas-fed burner.

Internal Indirect Reformer

- Heat is supplied by the exothermic reaction of the SOFC, but reforming does not occur on the cell anode. The reforming and SOFC reactions are thermally connected but spatially separated.

Internal Direct Reformer:

- The reforming reaction occurs directly on the anode of the fuel cell. To avoid localized hotspots and ensure optimal operation, only about 50% of the fuel should be reformed directly on the anode, with the remaining 50% reformed using the external or internal indirect methods

The SOFC model in Aspen Plus

To establish the Aspen Plus model for our process, we need to follow four main steps:

1. Component definition:
    - Identify and define all the components involved in the process. For our case, the relevant components are methane (CH_4), carbon dioxide (CO_2), nitrogen (N_2), oxygen (O_2), hydrogen (H_2), water (H_2O), and carbon monoxide (CO).
2. Equation of state selection:
    - Choose an appropriate equation of state for solving the thermodynamic properties of the system. In this study, we selected the Peng-Robinson equation of state due to its suitability for handling hydrocarbons and non-polar substances under a wide range of conditions.
3. Unit system configuration:
    - Configure the unit sets to define measurement preferences. For this analysis, the SI system will be employed, with exceptions for pressure and temperature, which will be specified in bar and degrees Celsius (°C), respectively.

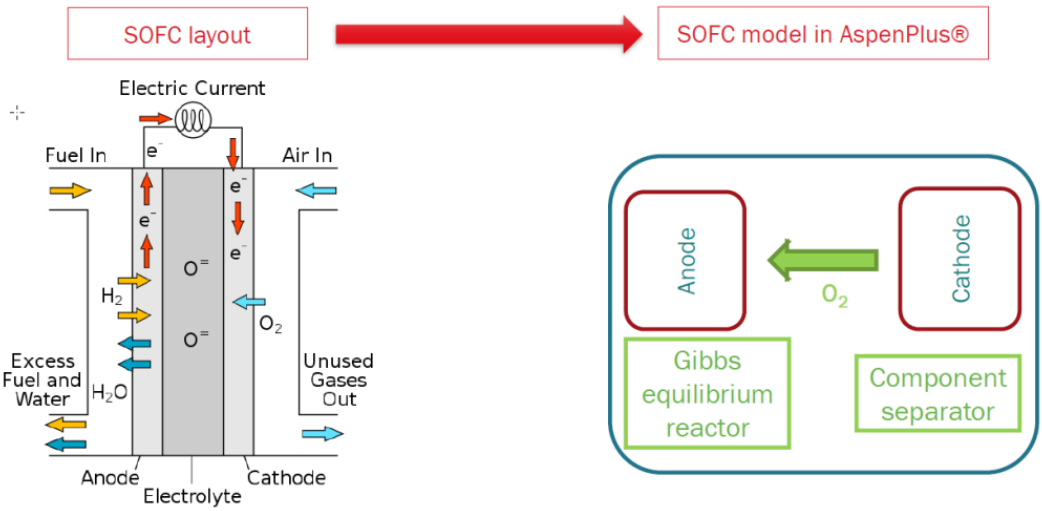

Figure 7. Schemes of a SOFC module (on the left) and of a SOFC model on AspenPlus

Biogas-fed Sold Oxide Fuel Cell stack modelled on Aspen plus

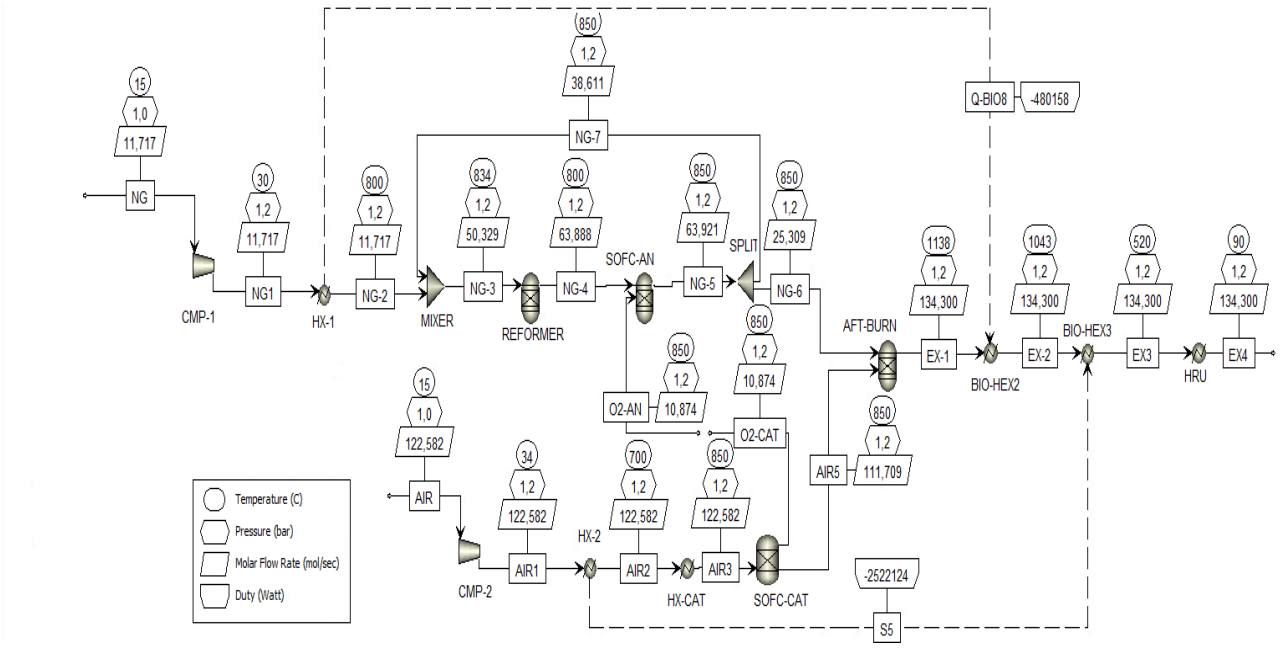

Figure 8. SOFC simulation on AspenPlus

The model for a biogas-fed Solid Oxide Fuel Cell (SOFC) stack developed in Aspen Plus involves several components, as the SOFC itself is not available as a single unit in the software. Consequently, a multi-component approach was adopted. The cathode is represented as a heat exchanger, which simulates the temperature increase of the air within it. Since the incoming air is slightly cooler than the fuel, this creates a temperature gradient that needs to be replicated using this fictitious heat exchanger.

The cathode also includes a fictitious separator that simulates the stoichiometric oxygen. This oxygen is separated from the cathode and transported to the anode through the electrolyte as oxygen ions. The anode is modelled as a Gibbs reactor, where the actual reaction between hydrogen and oxygen occurs. To manage the thermal balance, oxygen flows are modelled as separate streams. This separation is essential for performing a thermal balance on the anode (fuel line) before calculating the air flow required to cool the SOFC.

The modelling approach involves first solving the anode line to determine the heat to be removed. Subsequently, the air flow required for cooling is calculated. Direct connection of these components could lead to convergence issues; however, consistency between them is maintained. As illustrated in Figure 8, the anode and cathode are linked via the "O_2-AN" stream, representing the flux of O_2- ions from the cathode to the anode.

The inlet streams consist of biogas and air, which are initially processed by blowers to minimize pressure losses, with an assumed pressure drop of 200 mbar. Preheaters are used to elevate the temperature of these streams to the required inlet temperature using two heaters powered by hot exhaust gases. The air is then directed to the cathode, while the biogas undergoes partial or complete reforming into hydrogen before reaching the anode. This is necessary because direct use of pure methane could lead to undesired "cold spots" in the SOFC. Reforming is performed in a dedicated reactor using steam reforming. To avoid the high costs of external water, the steam required for reforming is sourced from the anode exhaust, which contains water and represents a more cost-effective option.

The exhaust gases from both the anode and cathode are sent to an afterburner. This chemical reactor combusts any unreacted fuels in the SOFC exhausts, addressing the fuel utilization (FU) percentage, which is less than 100%.

The chemical energy from the burned gases is converted into thermal energy, leading to an increase in temperature. This thermal energy is then utilized for preheating purposes and for thermal recovery within the plant before being released into the chimney.

In the Aspen Plus simulation, the Peng-Robinson equation of state was chosen as the base method for solving the gas phase equilibrium due to its suitability for modelling thermo-chemical processes involving gases and liquids. It is important to note that a zero-pressure drop is assumed for all components in the model.

- The blower between biogas streams 1 and 2 is modelled as an isentropic compressor with a discharge pressure of 1.2 bar. The simulation assumes isentropic compression with a mechanical efficiency of 90% and a volumetric efficiency of 80%.
- A reformer, specifically a Gibbs reactor, is used to minimize Gibbs free energy and achieve equilibrium. The heat required for the reformer is partially supplied by the heat generated by the SOFC. As detailed in the results section, while there has been a reduction in CO2 emissions, only a fraction of the methane has been converted to date; complete conversion of methane will be addressed subsequently. The reformer operates at a temperature of 750 °C, necessitating the inclusion of a preheater in the simulation to achieve the required operational temperature.

The initial input value for the amount of fuel is set to []. This value is crucial for calculations in the “flow sheeting options.” To facilitate accurate calculations, a hypothetical molar flow rate of 1 mol/s is initialized in the calculator. This allows for the proper adjustment of all subsequent flow values. The biogas composition is assumed to be 60% methane (CH4) and 40% carbon dioxide by mole fraction.

The first component encountered by the biogas in its pathway is the blower. Since Aspen Plus does not have a dedicated blower component, a compressor with a different pressure drop is used as a substitute, given that both are considered pressure-changing devices. An isentropic compressor type is selected, with a discharge pressure set to 1.2 bar, corresponding to a pressure increase of 200 mbar relative to the inlet pressure.

The subsequent component is the heater, which preheats the gas for the reforming process. The heater is set to achieve a temperature of 750 °C, the required operational temperature for the reformer. Pressure drops are influenced by the system's geometry and size, making it challenging to specify for all components. In this case, the pressure is set to zero, as Aspen Plus interprets values less than or equal to zero as pressure drops, while positive values are considered outlet pressures.

In the results section, the blower requires a power input of 617.4 W (brake horsepower). For the heater, the heat duty is recorded as a positive value, indicating the heat provided to the block. Although the source of this heat is not currently specified, it will later be considered as coming from the exhaust gases.

The heated biogas is directed to the reformer, where the conversion process requires the presence of water. Rather than sourcing water externally — which would incur additional costs, particularly for large-scale systems — the simulation utilizes steam generated from the SOFC anode exhaust. The reaction between hydrogen (H_2) and oxygen (O_2) in the SOFC also produces steam, which is collected at the anode outlet and used for the reforming process.

The reformer operates with a heat duty of 96,830 W, indicating an endothermic reaction, as the system absorbs heat. Some of the heat produced by the fuel cell will be used to supply this requirement. According to the Stream Results section, a significant portion of CH_4 and CO_2 is converted, with some H_2 and CO being produced. However, because this process is a dry reforming, additional water is required to fully convert all methane.

The next component in the simulation is the SOFC anode, modelled as another Gibbs reactor. This reactor has two inlet streams: one from the reformer and the other consisting of oxygen ions from the cathode. The operating temperature for the SOFC anode is set to 800 °C, which is typical for fuel cell operations. The oxygen-ion stream is defined with a molar fraction of 100% oxygen.

Before proceeding with further modelling, it is necessary to define and update the values for the biogas and oxygen inlet streams using Aspen Plus’s “flow sheeting option.” The Calculator will facilitate this by exporting variables from the calculator to the main flowsheet. Specifically, we need to define the following export variables: fuel molar flow rate, oxygen flow rate, and total current, which will be used later to calculate the total power production. For stability reasons, we will use the Fortran environment for these calculations. The required statements will be:

$$\dot{m}_{biogas}\left[\frac{kg}{s}\right] = \dot{V}_{biogas}\left[\frac{m^3}{s}\right] \cdot \rho_{biogas}\left[\frac{kg}{m^3}\right]$$

$$\dot{n}_{biogas}\left[\frac{mol}{s}\right] = \dot{m}_{biogas}\left[\frac{kg}{s}\right] \cdot \frac{1000\ \left[\frac{g}{kg}\right]}{3600\ \left[\frac{s}{h}\right]} \cdot MW_{biogas}\left[\frac{g}{mol}\right]$$

$$\dot{n}_{oxygen} = \frac{I_{tot}}{4 \cdot F}$$

$$z_{C_xH_yO_z} = 4 \cdot x + y - 2 \cdot z$$

$$I_{tot}[A] = \dot{n}_{biogas} \cdot y_{CH_4} \cdot z_{CH_4} \cdot F \cdot FU = \dot{n}_{CH_4} \cdot F \cdot FU$$

$$W_{DC_{gross}}[MW] = I_{tot} \cdot V_{op}$$

Where:

- $\dot{n}_{biogas}$ is the fuel molar flow rate defined within the block and exported to the flowsheet, in order to overwrite the initial value of 1 mol/s.
- I_{tot} is the total current produced from the available fuel flow rate according to the Faraday's law and considering the SOFC fuel utilization, which will be initialized in the calculator. This value is exported as a *PARAMETER* on Aspen since it is not linked to any block or stream within the flowsheet.
- $\dot{n}_{oxygen}$ is the stoichiometric amount of oxygen requested by the SOFC electrochemical reaction (Faraday's law). This value will be overwritten in the stream of oxygen fed to the anode.
- y_{CH_4} is the methane fraction (% mol.) in the inlet biogas stream.

Some of these values are obtained by means of the procedure below:

Parameter	Value
$\boldsymbol{\rho_{CH_4}}$	0,657 $\frac{kg}{m^3}$
$\boldsymbol{\rho_{CO_2}}$	1,87 $\frac{kg}{m^3}$
$\boldsymbol{MW_{CH_4}}$	16 $\frac{g}{mol}$
$\boldsymbol{MW_{CO_2}}$	44 $\frac{g}{mol}$

$$\rho_{biogas} = \boldsymbol{\rho_{CH_4}} \cdot y_{\boldsymbol{CH_4}} + \boldsymbol{\rho_{CO_2}} \cdot y_{CO_2}$$

$$MW_{biogas} = MW_{\boldsymbol{CH_4}} \cdot y_{\boldsymbol{CH_4}} + MW_{\boldsymbol{CO_2}} \cdot y_{CO_2}$$

Assuming a 60% mol. of $\boldsymbol{CH_4}$ content in biogas, 80% of fuel utilization FU (between 70% and 90%) and a Faraday constant F=96'485 C/mol, the fuel density will result as 1,2 $^{kg}/_{m^3}$ and the molecular weight 27,2 g/mol.

The results are reported in the Table 1 below.

$\dot{n}_{biogas}\ [mol/s]$	11,72
$\dot{m}_{biogas}[kg/s]$	0,33
$MW_{biogas}[g/mol]$	34,65
z_{CH_4}	8
FU	0,8
$F\ [C/mol]$	96'485
$V_{op}\ [V]$	0.8
$I_{tot}[A]$	4'187'500
$W_{DC_{gross}}[MW]$	3,35

Table 1. Results from Aspen model

In this way the biogas and oxygen molar flow rate values will be updated and overwritten on the *Main Flowsheet* and on the *Results* section. The next steps are related to the evaluation of the electricity injected in the grid, the efficiency of AC and DC electricity production, the thermal efficiency, and the total efficiency of the plant. The latters are evaluated with the following formula:

$$\eta_{el,DC} = \frac{W_{DC_{gross}}}{\dot{m}_{biogas} \cdot LHV_{biogas}}$$

$$\eta_{el,AC} = \frac{W_{AC_{net}}}{\dot{m}_{biogas} \cdot LHV_{biogas}}$$

$$\eta_{th} = \frac{Q_{HRU}}{\dot{m}_{biogas} \cdot LHV_{biogas}}$$

$$\eta_{tot} = \eta_{el,AC} + \eta_{th}$$

$W_{AC_{net}}$ was evaluated by considering the inverter efficiency equal to 0.95 and subtracting the electrical consumption of the two compressors. The results are reported in Table 2.

$W_{AC_{net}}\ [MW]$	3,1
$\eta_{el,DC}$ [-]	0,615
$\eta_{el,AC}$ [−]	0,568
$\eta_{th}[-]$	0,342
η_{tot} [−]	0,911

Table 2. Efficiencies of the plant

We are still missing the recirculation loop, so the reformer is not having water at the inlet because we need to take part of the steam of the exhaust mixture and send it back to the reformer to provide enough steam for the reforming. In order to do this, we first need to split the outlet of SOFC-AN into two sub streams by means of a splitter component. As a split fraction we choose 0.5, so that the 50% of the exhausts is expected for the recirculation. In the reformer stream results we can see that at the inlet we have some water, but also some hydrogen and CO because there is always a small amount of unreacted fuel which is recirculated back. At the outlet water will be consumed while hydrogen and CO are produced, so their flowrate increased. What is still not correct is that we want to operate the reformer with the steam-to-carbon of 2, where the latter is defined as $SC = \frac{\dot{n}_{H2O}}{\dot{n}_{CH4}}$, so the ratio between the water content at the inlet of the reformer and the methane one in molar basis. An SC of 2 of course means to have a double amount of water with respect to methane: in order to reach this goal, we'll develop an objective function where we'll impose to change the split ratio (initialized with 50% before), such that SC is set to 2,5. The tool used for this kind of calculation is the *Design Specifications*. Since it is mandatory to set a tolerance, we will choose 0,01. The percentage of recirculated gas will be decided inside the split block, following the manipulated variable limits (between 0 and 1), achieving its optimal value. Finally, after running the simulation, we can state that for a Steam-to-Carbon of 2 we need to recirculate the 58% of the anode exhausts. Now H2 and CO are reduced, very near to 0 amount even if not completely due to the fuel utilization FU, thanks to the reaction which now took place with oxygen, therefore producing water and CO2.

Now we can move to the definition of the cathodic line. We'll define the inlet air at ambient conditions, exactly as we did for the biogas stream. The molar flowrate is again initialized, but then it will depend on the thermal balance of the system: in other words, the SOFC is exothermic, so it is producing heat, while the reformer is endothermic, so it requests heat; the SOFC heat production goes to the reformer and the remain heat produced will be removed by the air. We won't put 1 mol/s as a first try because we already set it for the oxygen stream, so in order to not receive errors from the simulation, we'll set something more like 10 mol/s. We implemented the typical composition of air that is 21% of oxygen and 79% of nitrogen. An air blower is needed, and we put the exact same properties as the ones chosen for the biogas' blower. The next component is the heat exchanger for pre-heating purpose: the chosen temperature is in fact the one at which the air is entering the cell, so 650°C, in fact since we want to remove the heat in the SOFC, we need to create a gradient temperature across it. With a $\Delta T = 150°C$ across the cathode, the air will remove the excess heat produced by heating up. Another heater will be used for simulating the temperature increase of the air inside the stack, so this is just a fictitious component: for these reasons we'll set a temperature of 800 °C for the sensible heat requested to heat up the stream. Then a separator is needed to divide the stoichiometric oxygen going to the anode from the whole stream: this will represent in a certain way our cathode side of the SOFC, along with the CAT-HX. There will be two outlets: the first for the exhausts in the plant and the second for the oxygen going in the anode. The stream O2-CAT is in fact simulating the flow of oxygen ions going from the cathode to the anode side, but because of Aspen convergency we can't put all in a unique stream, therefore we have to build them separately as explained before. In the SOFC-CAT block we impose a 0-split fraction for

nitrogen, in order to have it all on the other side; for what concerns the oxygen amount, 1 mol/s as initialization value is fine; all the rest will automatically go in the other stream. Now we need to build a calculator in order to tell Aspen that O2-CAT coincides with O2-AN: first we need to import the amount of oxygen at the anode, calculated before, from the flowsheet to the calculator, and then to export the O2 extracted from the cathode; the only information to be written on Fortran is $\dot{n}_{O_2,anode} = \dot{n}_{O_2,cathode}$. By running the simulation we'll notice that the molar flow rates are now the same, 1,09 mol/s.

We can also observe that the amount of heat requested by the reformer SOFC-CAT is about 170 kW, while for SOFC-AN the amount is negative: the value indicated is the enthalpy change across the anode, which is not all going into heat: because of the first principle of thermodynamics, ΔH_{anode} is partially provided for electricity production and the remaining part for heat, so we need to make this calculation. The difference between how much it is produced and how much goes to the reformer is the heat that has to be removed by the air, which is the heat of CAT-HX. We need to build a calculator for this purpose in order to know how much heat should be removed by air. The information to be implemented are:

- the enthalpy changes across the anode to be imported.
- the current calculated previously as an import variable.
- the heat requested by the reformer, which is already available in the block, so it's an import variable.
- the electric power produced which has to be obtained in the calculator environment and then exported.
- the waste heat which has to be removed by air.

$$|\Delta H_{reac}| = |\Phi| + |W_{el}|$$

$$|\Phi| = |\Delta H_{reac}| - |W_{el}| = |\Delta h| \cdot \dot{n}_{H_2} - V_C \cdot I_{tot} = |\Delta h| \cdot \frac{I \cdot n_{cell}}{2F} - V_C \cdot I \cdot n_{cell} =$$

$$= I \cdot n_{cell} \cdot \left(\frac{|\Delta h|}{2F} - V_C \right)$$

In this model, we will not develop the full electrochemical model, including activation, polarization, and ohmic losses, or the Nernst potential. Instead, we will assume the operating voltage is known and fixed at 0.8 V. Based on this assumption, the electrical power generated can be calculated as the product of the total current and the operating voltage.

The excess heat produced by the system is determined by the difference between the total enthalpy change across the solid oxide fuel cell (SOFC) and the electrical power output. This excess heat represents the irreversible heat generated during operation. It is important to note that the enthalpy change, ΔH_{reac}, is negative, as it represents energy leaving the system. Therefore, to calculate the total heat produced in absolute terms, we must account for the sign of ΔH_{reac} by adding a negative sign in front of it. The total heat produced by the fuel cell is thus:

$$Q_{total} = -\Delta H_{reac} - P_{elec}$$

The waste heat that must be removed by the air is calculated as the total heat produced minus the heat absorbed by the reformer. Since the reformer operates via an endothermic reaction, the heat it absorbs is positive. Therefore, the total heat removed by the air is:

$$Q_{air} = Q_{total} - Q_{reformer}$$

In our case, the electrical power generated is approximately 337 kW, the total enthalpy change across the SOFC is 559 kW, the heat required by the reformer is 170 kW, and the waste heat to be removed by the air is 50 kW.

Next, we instruct Aspen to ensure that the heat removed by the cathode-side heat exchanger matches the waste heat value we have just calculated. Our goal is to set the net duty of the cathode heat exchanger ($Q_{hex\ air}$) to 50 kW, which can be achieved by adjusting the air flow rate. To accomplish this, we will use the design specification feature in Aspen. We set the target as:

$$Q_{waste} - Q_{hex\ air} = 0$$

with a tolerance of 0.1 kW. The air flow rate will be the variable adjusted to meet this target. The minimum air flow rate will correspond to the stoichiometric oxygen requirement, ensuring sufficient oxygen for the reaction. This is determined by dividing the required oxygen by 0.21, accounting for the oxygen content in air. The maximum air flow rate will be set at 20 times the minimum value, providing a wide range for adjustment, ensuring that the simulation remains robust, even when scaling the plant size, as the variable limits will adjust accordingly.

The last step is to import the parameters Q_{waste} and $Q_{hex\ air}$ into the model as block variables. Additionally, we will later introduce another stream variable, the oxygen flow rate to the anode ($O_{2\ anode}$), for further analysis.

In this way we have correctly modelled all the SOFC system, until the anode and cathode exhausts. The last part will be the heat recovery section.

In our process, we still have unreacted components such as H2 and CO. We will utilize a burner to combust these gases, which will be modeled using again a Gibbs equilibrium reactor. Unlike the previous reactors, which were modeled as isothermal, the burner will be considered adiabatic since we do not want to set a specific temperature. Thus, all the heat generated by the reaction will contribute to an increase in temperature, and the heat duty will be set to zero. Upon running the simulation, a significant temperature rise is expected, from 800°C to 1240°C, even if, in practice, cooling systems might be necessary to prevent excessively high temperatures that could damage materials such as alloys, thus limiting the actual achievable temperature.

After the complete combustion of H2 and CO, CO2, water, and steam are produced, with some oxygen consumption. The very hot stream exiting the burner will be used for preheating the inlet stream. To achieve this, we will connect the biogas heat exchanger and the air heat exchanger, and we will also utilize the *Q-AIR* stream for preheating the air. Additionally, we will incorporate a Heat Recovery Unit (HRU). The cooling temperature of the exhaust in the HRU will be set to 80°C, considering that the exhausts are not in a condensing state at this point. This cooling temperature may vary depending on the specific application of the plant; for instance, some plants may prefer to produce steam and avoid excessive cooling of the exhaust.

With these considerations, the Aspen model can be considered complete.

Methods and modelling

4.1 Theoretical Description of the Key Topics: Syngas and H_2S

4.4.1 Syngas (Synthesis Gas)

Syngas, short for synthesis gas, is a mixture of gases primarily composed of hydrogen (H_2), carbon monoxide (CO), and in some cases, carbon dioxide (CO_2). It is produced through gasification processes, typically by reacting carbon-containing materials—such as biomass, coal, or natural gas—with oxygen (or air) and steam at high temperatures. The result is a combustible gas that can be used in various industrial applications, including electricity generation, chemical synthesis, and as a feedstock for producing hydrogen or liquid fuels.

In the context of biomass gasification, the syngas produced is typically rich in hydrogen and carbon monoxide, both of which are crucial for energy production. The main reactions involved in gasification include:

- Partial oxidation of carbon: $C + \frac{1}{2}O_2 \rightarrow CO$
- Steam reforming of hydrocarbons: $CH_4 + H_2O \rightarrow CO + 3H_2$
- Water-gas shift reaction: $CO + H_2O \rightarrow CO_2 + H_2$

Syngas has a lower energy content compared to natural gas, but it can be efficiently used in combined heat and power (CHP) systems or further processed in Solid Oxide Fuel Cells (SOFCs) for electricity production. The key advantage of using syngas in these systems is the flexibility it offers, allowing for the integration of renewable biomass as a fuel source. However, syngas must often undergo gas cleaning processes to remove impurities like tar, particulates, and acidic gases, which can damage equipment and reduce system efficiency.

4.1.2 Hydrogen Sulphide (H_2S)

Hydrogen sulphide (H_2S) is a colourless, toxic gas with a characteristic smell of rotten eggs. It is a common contaminant found in syngas produced from biomass gasification, particularly when the feedstock contains sulphur compounds. Even in small concentrations, H_2S can

cause significant problems in energy systems like fuel cells, as it can poison the catalysts used in SOFCs and other technologies. This necessitates the removal of H_2S to very low levels, often below 1 ppm, before the syngas can be used efficiently.

The typical reactions involving H_2S in gas-cleaning systems include its removal through adsorption or chemical reactions with sorbents. Zinc oxide (ZnO) is one of the most widely used materials for H_2S removal, operating according to the following reaction:

$$ZnO + H_2S \rightarrow ZnS + H_2O$$

In this reaction, the hydrogen sulphide reacts with zinc oxide to form zinc sulphide (ZnS) and water, thus purifying the gas stream. The use of ZnO is advantageous due to its high capacity for sulphur and the fact that it works well in the high-temperature environments typical of gasification processes.

Efficient removal of H_2S is critical not only for protecting equipment but also for ensuring that the syngas can be utilized in CHP or SOFC systems without causing degradation, thus aligning with the objectives of projects like Micro-Bio-CHP, where minimizing emissions and improving the efficiency of biomass-based energy systems are key priorities.

4.2 Adsorption Process

HYSYTECH's role in this project is to develop and optimize the section for the removal of HCl and H_2S. This involves the design of two reactors with different adsorbents capable of selectively removing these substances. The reactors are required to operate continuously for at least one year. Additionally, HYSYTECH will be responsible for designing and constructing a laboratory-scale plant to test the adsorbents under various operating conditions and to evaluate the reactor design. The results from these tests will be used for scaling up the reactor to the desired size, followed by integrating the removal section with the SOFC.

The two reactors will be sized based on the state-of-the-art adsorbents used for these purposes: K_2CO_3 for HCl removal and ZnO-based adsorbents for H_2S removal.

They were designed to follow the compactness and pressure drops requirements. The design is chosen to be a U-shape reactor which will have the two sorbent beds in the straight sections, so one for the HCl and the other for H2S removal: this solution assures the desired compactness, aside from an easy-to-replace sorbents procedure. The pressure drop of the reactor was evaluated to be around 10 mbar. The preliminary design will be executed by Hysytech and then delivered to the partners for a first stage testing of the Micro-Bio-CHP concept.

4.2.1 Objectives

The MBC concept is about a biomass fixed-bed updraft gasifier that is directly coupled with a gas burner and boiler in order to produce heat. Furthermore, a gas extraction is needed to feed product gas to a solide oxide fuel cell system for electricity production too. In Figure N is shown the block-flow diagram of this overall concept. With the latter, the exhausts extracted from the gasifier and directed to the SOFC are subjected to some treatments:

1. Tar reforming
2. Soot particle removal
3. HCl and H2S removal

We will focus on the third point which has to be integrated into the SOFC module: this will include the preliminary sizing, the geometry of the reactor and the specifications of the sorbents to be used.

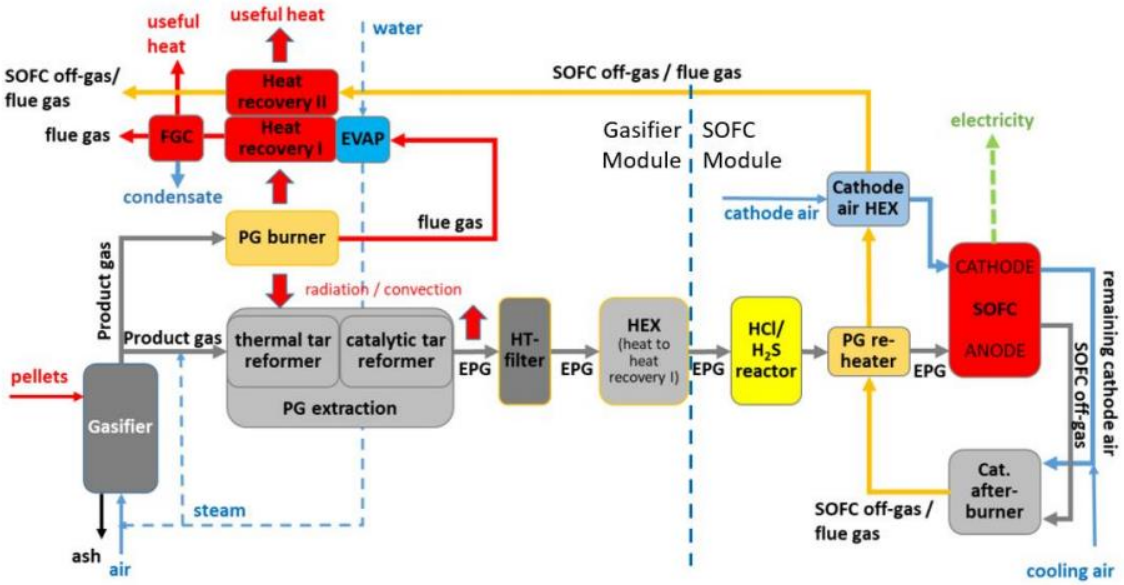

Figure 9. Basic design of the MBC system

4.4.2 Absorption Phenomena in Filtration

The behavior within a filter is governed by the phenomenon of absorption. Absorption refers to the variation in concentration of a particular substance between the interface and the adjacent phases. [11]

Absorption can be classified based on the phases involved and the type of separation:

- **Absorption** occurs when both phases involved are fluids.
- **Adsorption** occurs when at least one phase is solid.

Adsorption can be defined as the process where one or more substances (the adsorbate) adhere to the surface of a solid (the adsorbent) through the formation of weak or strong bonds. In this context, the acidic gases are the substances to be adsorbed, with the process gas being the fluid. The objective of adsorption is to retain these acidic gases by trapping them within or on the surface of the solid adsorbent.

Adsorption itself can be further categorized into two classes, depending on the nature of the interactions between the fluid and the solid:

- **Physisorption** involves intermolecular bonds, such as Van der Waals, London, or Debye forces. These bonds are relatively weak, making them easily reversible and allowing for the regeneration of the adsorbent due to the low enthalpy of formation.
- **Chemisorption** involves intramolecular bonds, such as ionic or covalent bonds. This type of adsorption is driven by a chemical reaction, characterized by a high enthalpy of formation and generally considered irreversible.

Chlorinated Compounds Removal

Chlorinated compounds are removed from gas streams through a dehydrohalogenation process using metal oxides or carbonates.

Among the various technologies for HCl removal, hot washing with either fixed or fluidized beds is highly versatile with respect to both temperature and operational pressure. For these removal technologies, solid "catalyst-adsorbents" have been developed with high sorption capacity, defined as the amount of HCl adsorbed and reacted per unit mass of adsorbent. These adsorbents must also demonstrate durability under the operational conditions of the equipment, including high pressure, elevated temperature, and particle attrition. Metal oxides supported on alumina, such as CaO, MgO, and K_2O, are among the most commonly used adsorbents. These materials react with HCl to form the corresponding metal halides.

Once the chloride forms on the adsorbent surface, regeneration in its oxidized form becomes challenging, particularly given the energy requirements for chemisorption, which are significantly higher than those for physical adsorption. Among metal oxides, K_2CO_3 has been found to be the most effective adsorbent for HCl within the operational range for cleaning Product Gas. The primary reaction is:

$$K_2CO_3 + 2HCl \rightarrow 2KCl + CO_2 + H_2O$$

Literature suggests that optimal operating conditions are 20 bar and 400 °C.

4.3 Properties

Hot gas cleaning seems the most suitable way for this process: it has the advantage of increasing the efficiency of the process which requires a high temperature for the exhausts to be used as in this contest. By consulting previous project materials, a temperature range between 300 °C and 400 °C can be appropriate for this purpose, of course using proper sorbent materials for the removal of HCl and H2S. The inlet specifications are summarized in Table 3 below.

Table 3 H2S/HCl removal reactor inlet conditions

Parameter	UOM	Value at full load	Value at partial load
Temperature	[°C]	400	300
Volume flow	[Nm^3/h	4.66	2.33
Mass flow	[kg/h]	3.98	1.99
Gas composition			
CO	[wt% w.b.]	18.48	18.48
H_2O	[wt% w.b.]	27.66	27.66
CO_2	[wt% w.b.]	26.77	26.77
H_2	[wt% w.b.]	3.14	3.14
N_2	[wt% w.b.]	23.94	23.94
H_2S	[wt% w.b.]	0.0030	0.0030
HCl	[wt% w.b.]	0.0021	0.0021
CO	[vol% w.b.]	12.65	12.65
H_2O	[vol% w.b.]	29.43	29.43
CO_2	[vol% w.b.]	11.66	11.66
H_2	[vol% w.b.]	29.87	29.87
N_2	[vol% w.b.]	16.38	16.38
H_2S	[ppmv w.b.]	16.90	16.90
HCl	[ppmv w.b.]	11.06	11.06

The H2S and HCl concentrations of the product gas have been assessed based on transfer factors calculated for S and Cl from the fuel to the product gas obtained by the consultation of the papers of other projects: the S and Cl contents of the fuel, which in our case consists in wood pellets, represent database mean values plus the standard deviation. Thus, H2S and HCl contents we considered are on the safe side.

The reactor should remove H2S and HCl to a proper level for the SOFC module. A reasonable level is to obtain a clean gas with a maximum content of 1 ppm; the reactor will be also projected in order to change the sorbent every 3000 hours of operation at full load.

4.4 General methods

Adsorption process can be described by means of the mass-transfer zone concept. Due to the high concentration of contaminants the sorbent closer to the inlet of the fluid saturates quicklier, and a saturated zone called equilibrium zone is formed. After the latter, the profile of the contaminant concentration shows a concentration gradient, and once it is stable and completed it assumes the typical S-shape profile. The region of the bed where this kind of profile is present is linked to the mass transfer zone (MTZ). MTZ moves along the bed in the same direction of the gas flow since the sorbent is being depleted during the process. Its

shape is the result of the superposition of the bulk and pore diffusional resistances, adsorption, and reaction kinetics.

An extremely low level of concentration of the contaminant is guaranteed at the outlet of the column since the contaminant reacting on the solid starts the saturation or depletion. The breakthrough begins when the edge of the MTZ reaches the bottom of the bed, thus the concentration of the contaminant starts to increase.

4.4.1 Shrinking Core Model – SCM

It is exploited to simulate the consumption of a solid particle by the reaction with a gaseous reactant, as well as for the calculation of the radial position of the reaction zone interface for each point of the discretization.

This model is a simplification of the Progressive-Conversion Model.

The reaction first happens at the more external layer of the particle, then it moves inside the solid, leaving behind a layer of inert (reacted material) called “ash”.

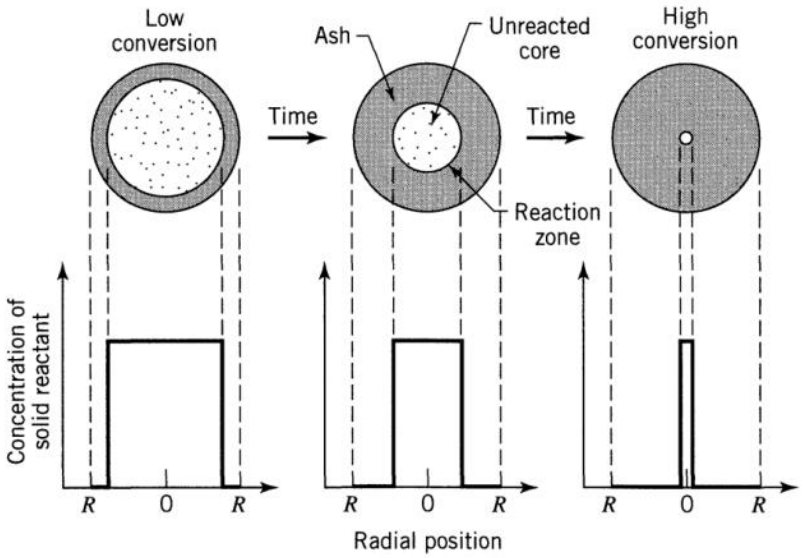

Figure 10. Shrinking core model concept

The two reactions taking place for the HCl and H2S removal are:

$$K_2CO_3 + 2HCl \rightarrow 2KCl + CO_2 + H_2O$$

$$ZnO + H_2S \rightarrow ZnS + H_2O$$

Thus, we can state that the ash layer, in this case, will be made of KCl and ZnS for the first and for the second reaction respectively.

The reaction between a reacting solid particle and surrounding gas phase can be described as:

1) Diffusive transport of gaseous reactants through the gas film at the particle surface
2) Diffusion of gaseous reactants through ash or the product layer surrounding the unreacted core
3) Reaction of gas and solid at the reaction site
4) Diffusion of gaseous reaction products from the reaction site to the particle surface
5) Diffusion of gaseous products from the particle surface to the surrounding bulk flow

It has been proven that the total mass of the sorbent remains constant during the occurrence of the reaction: thus, the solid product is stuck on the particle producing a higher resistance to the diffusion of the sorbate with respect to the surrounding film.

Moreover, the reaction is modelled as an instantaneous one thanks to the favourable conditions.

The sorbent materials used for the modelling of the system are HTG-10 ($K_2CO_3, > 20\%\ wt$ with Al_2O_3 as support) and HTZ-5 ($ZnO, > 99\%\ wt$).

Topsoe chlorine absorbent, HTG-10, is used for the removal of hydrogen chloride. Organic compounds containing at least one covalently bound chlorine atom must be first be hydrogenated into inorganic chloride via Haldor Topsoe TK catalyst in order to be removed by HTG-10. It is recommended installing it upstream the zinc oxide absorbent in order to prevent the formation of zinc chloride. The absorbent is supplied in steel drums containing 200 litres nominal capacity; a polyethylene bag inside the drums protects the absorbent from moisture while the drums are fitted with a removable lid.

Finally, from all these assumptions we started the computation of a MATLAB model, with the main goal of obtaining a breakthrough curve for the substances to be removed, according to the following steps:

1. Discretization of the control volume of the reactor, using the size of the column and the particle
2. Implementation of the SCM to calculate the radial position of the reaction zone interface for each point of the discretization:

$$\frac{dr_c}{dt} = -\frac{\upsilon_B \cdot D_e \cdot C_A \cdot M_B}{\upsilon_A \cdot \rho_B} \cdot \frac{1}{r_c - {r_c}^2/_R}$$

Where:

- r_c is the unreacted core radius
- υ_A and υ_B are stoichiometric coefficients (the gaseous reactant is represented by A, while the solid one by B)
- Molecular weight of B
- D_e is the effective diffusivity, represented in turn by the equation $D_e = \frac{\varepsilon_P}{\tau} D_{KA}$, where ε_P is the particle voidage (or porosity), τ the tortuosity, while D_{KA} represents the Knudsen (or binary) diffusion: $D_{KA} = \frac{d}{3}\sqrt{\frac{8RT}{\pi M_A}}$ (where d is the pore diameter).

3. The mass flux through reaction zone and mass balance at each point of the discretization:

$$C_A^{k+1} = C_A^k \cdot \left(1 - \frac{4\pi D_e}{\left(\frac{1}{r_c} - \frac{1}{R}\right)\dot{V}}\right)$$

Where:

- C_A^{k+1} is the concentration of the gaseous reactant A at the position k+1
- C_A^k concentration of the gaseous reactant A at the position k
- $\dot{V}$ volumetric flowrate of the gaseous reactant

The differential equations are solved with the ode45 function of MATLAB.

The analyser will show its own BT curve, which will have to coincide with the one of the Matlab model we created: if they don't, I will need to update the value of diffusivity with the one indicated by the analyser, since at the beginning it was just estimated.

4.5 Preliminary results

This sorbent material can easily reach 3000 hours of usage. Further improvements will be made after the construction of the reactor on a laboratory scale in order to fit the model with the actual diffusivity of the reactants, with particular attention to the variation in temperature and flowrate, since diffusivity strongly depends on them. In Table 4 you find the summarize of the parameters used:

Table 4. HCl and H2S data used for the shrinking core model

HCl Removal		
Temperature	400	°C
D_e	8.89E-06	m^2/s
ρ_B	1500	kg/m^3
R	2	mm
ν_B/ν_A	2	-
M_B	138.205	kg/kmol
$\dot{V}$ (total load)	4.66	m^3/h
$\dot{V}$ (partial load)	2.5	m^3/h
Column Diameter	110.3	mm
Mass fraction of sorbent	0.2	-
Active Column Height	400	mm
C_{HCL}	11	ppm

H_2S Removal		
Temperature	400	°C
D_e	4.31E-06	m^2/s
ρ_B	1900	kg/m^3
R	2.05	mm
ν_B/ν_A	1	-
M_B	81.38	kg/kmol
$\dot{V}$ (total load)	4.66	m^3/h
$\dot{V}$ (partial load)	2.5	m^3/h
Column Diameter	110.3	mm
Mass fraction of sorbent	1	-
Active Column Height	430	mm
C_{H2S}	17	ppm

In Figure 11 and 12 you find the breakthrough curve by means of the SCM for HCl and H2S respectively.

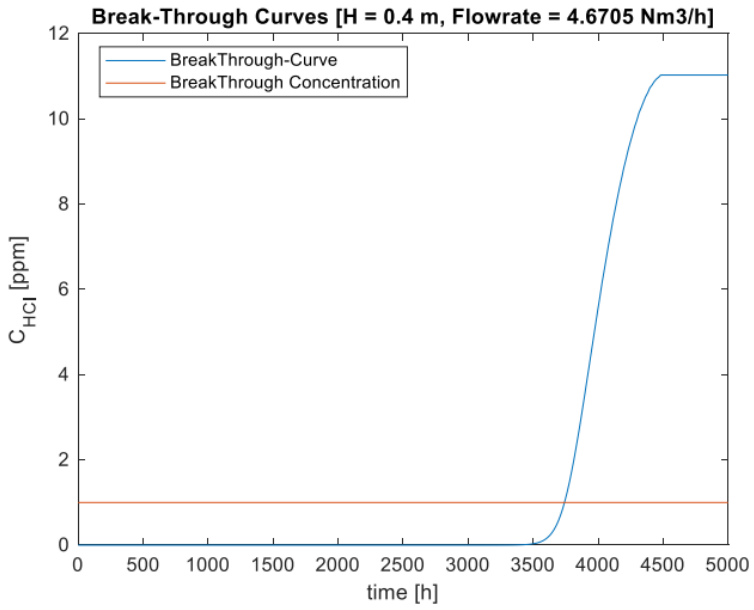

Figure 11. SCM breakthrough curve obtained for the HCl sorption

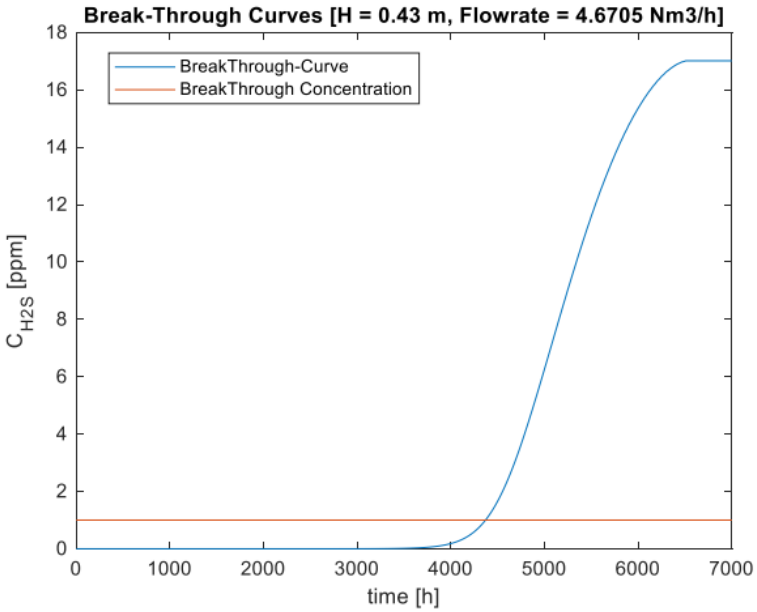

Figure 12. SCM breakthrough curve obtained for the H2S sorption

In this second case the reactor seems to be oversized with respect to the system, lasting in fact up to 4000 hours, since the sorbent material consists of mainly pure zinc oxide.

4.6 Testing plan for lab-scale HCl and H2S removal

The Fractional Factor Design was adopted, which allows the variation of several parameters to capture their effect on the system while maintaining a low number of tests. The parameters of interest are temperature, flowrate, concentration of the contaminant and the gas matrix composition, which are better described on Table 5.

Table 5. Varied parameters and ranges

Parameter	Temperature	Flowrate	Concentration	Composition
ID	A	B	C	D
Unit	°C	Nm^3/h	ppm	-
0 (Low Value Level)	300	0.75	30	N_2 + HCl/H_2S
1 (Medium Value Level)	350	1	50	N_2+CO_2+H_2+HCl/H_2S
2 (High Value Level)	400	1.25	100	N_2+CO_2+H_2+H_2O+HCl/H_2S

The gas composition for three tests is reported on table 6. These compositions were picked in order to study the effects of different gases on sorbent capacity. The composition indicated on the first column is the contaminant in inert gas, on the second there's the dry product one and the last one indicates the wet product gas since there's water. Carbon monoxide cannot be used in the test due to laboratory restrictions at Hysytech, therefore CO will be substituted by N2. We don't expect the formation of further gases.

Table 6. Gas compositions for the three tests

Component	N_2 + HCl/H_2S	N_2+CO_2+H_2+HCl/H_2S	N_2+CO_2+H_2+H_2O+HCl/H_2S
N_2	99.997% vol	58.47% vol	51.27% vol
H_2	0.00% vol	29.87% vol	29.87% vol
CO_2	0.00% vol	11.66% vol	11.66% vol
H_2O	0.00% vol	0.00% vol	7.20% vol
HCl/H_2S	30/50/100 ppmv	30/50/100 ppmv	30/50/100 ppmv

We can obtain a total of 81 tests if they're performed by varying one of these parameters at a time, but the total number of useful tests has been actually decreased to nine, which can be summarized in the Table 7 below.

Table 7. Test conditions

# TEST*	T (°C)	V (Nm^3/h)	C (ppm)	Composition
1	300	0.75	30	N_2
2	300	1	50	N_2+CO_2+H_2
3	300	1.25	100	product gas
4	350	0.75	100	N_2+CO_2+H_2
5	350	1	30	product gas
6	350	1.25	50	N_2
7	400	0.75	50	product gas
8	400	1	100	N_2
9	400	1.25	30	N_2+CO_2+H_2
*Test order should be randomized				

4.7 Piping and Instrumentation Diagram

In the attached Piping and Instrumentation Diagram (P&ID), we observe a detailed process flow system that is likely part of an industrial gas or liquid processing unit. It also contains key elements essential for the control and operation of a complex process system, including vessels, heat exchangers, control valves, and instrumentation that ensure safe and efficient operations. I will provide a short overview and highlight important aspects based on a general analysis of the diagram.

The process flow begins at the top left, where fluid enters through a feed stream, passing through several valves and instrumentation before reaching the heat exchanger. This system contains multiple inline instruments, such as flow transmitters (FT), pressure transmitters (PT), and level transmitters (LT), each designed to measure and transmit data related to the fluid's properties such as flow rate, pressure, and level. Furthermore, there is considerable instrumentation represented across the system, which indicates a high level of automation and control. The control loops include Pressure Control Loops, which maintain system pressure within specified limits, likely protecting the equipment from overpressure situations; flow control loops, that ensure the process fluid moves at the correct rate to maintain system efficiency; level control loops, particularly around the vessel, these loops ensure that the liquid level in the vessel is maintained to avoid overflows or dry runs.

All these control systems are also tied to alarms and emergency shutdown systems, ensuring safe operation under all conditions.

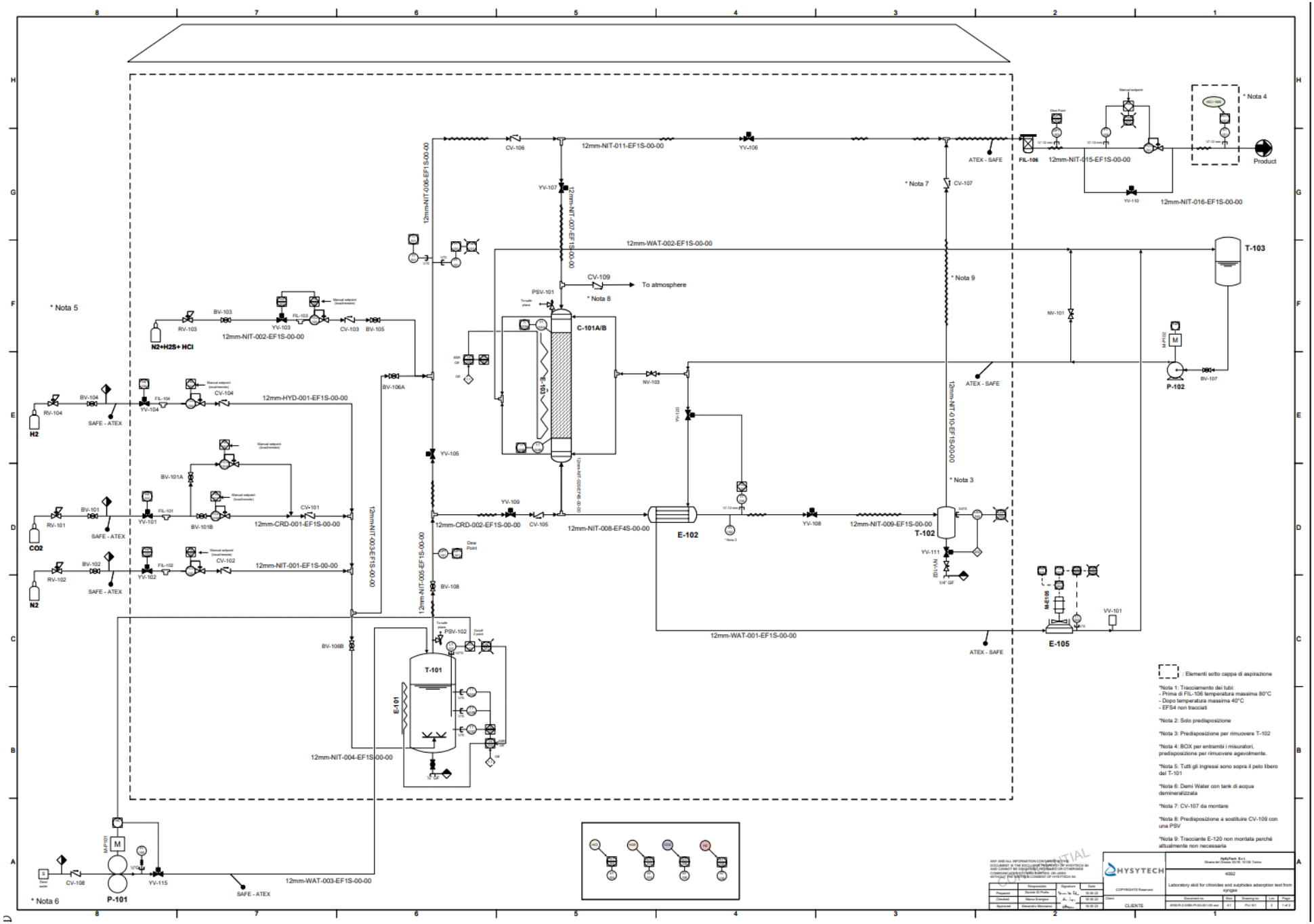
* Nota 5
N2+H2S+ HCl
H2
CO2
N2
SAFE - ATEX
12mm-NIT-002-EF1S-00-00
12mm-HYD-001-EF1S-00-00
12mm-CRD-001-EF1S-00-00
12mm-NIT-001-EF1S-00-00
12mm-NIT-003-EF1S-00-00
12mm-NIT-005-EF1S-00-00
12mm-NIT-006-EF1S-00-00
12mm-NIT-011-EF1S-00-00
12mm-NIT-007-EF1S-00-00
12mm-WAT-002-EF1S-00-00
CV-109
To atmosphere
* Nota 8
* Nota 9
* Nota 7
* Nota 4
* Nota 3
* Nota 6
C-101A/B
E-101
E-102
E-105
T-101
T-102
T-103
P-101
P-102
FIL-106
12mm-NIT-015-EF1S-00-00
12mm-NIT-016-EF1S-00-00
Product
12mm-CRD-002-EF1S-00-00
12mm-NIT-008-EF4S-00-00
12mm-NIT-009-EF1S-00-00
12mm-NIT-010-EF1S-00-00
12mm-WAT-001-EF1S-00-00
12mm-NIT-004-EF1S-00-00
12mm-WAT-003-EF1S-00-00
ATEX - SAFE
Elementi sotto cappa di aspirazione
*Nota 1: Tracciamento dei tubi:
- Prima di FIL-106 temperatura massima 80°C
- Dopo temperatura massima 40°C
- EFS4 non tracciati
*Nota 2: Solo predisposizione
*Nota 3: Predisposizione per rimuovere T-102
*Nota 4: BOX per entrambi i misuratori, predisposizione per rimuovere agevolmente.
*Nota 5: Tutti gli ingressi sono sopra il pelo libero del T-101
*Nota 6: Demi Water con tank di acqua demineralizzata
*Nota 7: CV-107 da montare
*Nota 8: Predisposizione a sostituire CV-109 con una PSV
*Nota 9: Tracciante E-120 non montata perché attualmente non necessaria
HYSYTECH
COPYRIGHTS Reserved
CLIENTE
4002
Laboratory skid for chlorides and sulphides adsorption test from syngas
4002-PJ-3080-PI-00-001-08.vsd
PU-101

Refrigeration Cycle

First Simulation in AspenPlus

In the initial simulation conducted in Aspen Plus, tank T-102 was modeled as a flash block capable of separating the vapor component from the liquid one. The incoming gas mixture consists, in molar percentage, of 51% N2, 29% H2, 7% H2O, and 13% CO2; the mixture is at a temperature of 35 °C with a vapor quality of about 65%.

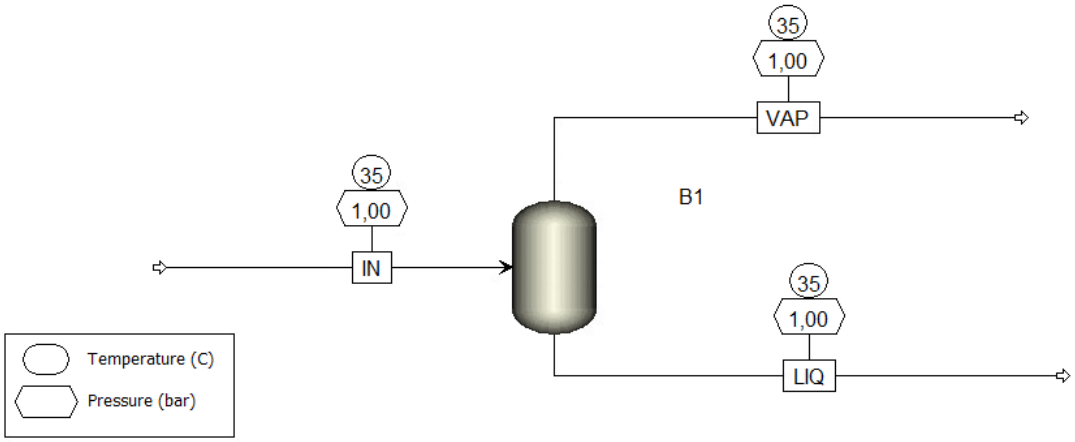

Figure 13. First simulation

We used the refrigerator already available in the company to collect the necessary data for implementation in Aspen Plus, aiming to analyze the outlet temperatures from the heat exchanger. The incoming gas, with the specified molar fractions, was considered as the hot fluid, while the refrigerant used was R1270, according to the manual specifications. R1270, also known as propylene, is a natural refrigerant belonging to the hydrocarbon category. Its properties include low environmental impact, practically zero global warming potential (GWP), and good energy efficiency. However, the simulation showed that the outlet temperature was too high. Previously, using only water as the cold fluid, we had obtained an outlet temperature of around 35 °C. Therefore, a different approach was necessary.

Second Simulation Method

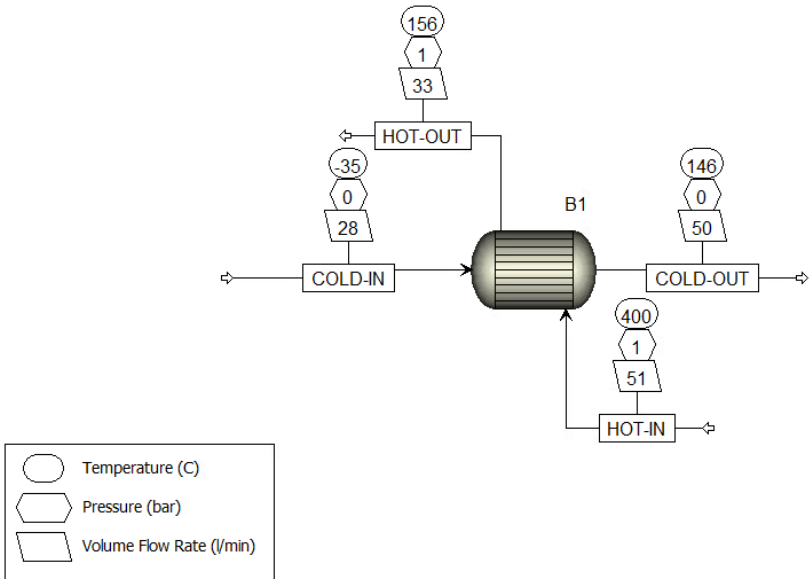

Figure 14. Second simulation

In the second method, as we can see from Figure 14, we implemented a primary heat exchanger using the initial configuration, a counterflow heat exchanger where water cools the gas. The gas, cooled from 400 °C to 42 °C, is further cooled using a thermostatic bath, modeled in Aspen Plus as a heater that utilizes the properties of the R1270 refrigerant.

In this configuration, water enters the heat exchanger at 24 °C, a temperature chosen to ensure the hot gas exits below the dew point, achieving a vapor quality of 100%. The water exiting the heat exchanger increases by only 2.5 °C, reaching 26 °C, and is then cooled in the thermostatic bath, dropping to 16 °C. This simulation allowed us to achieve an outlet temperature below 25 °C, enabling the installation of the already purchased refrigerator.

This new circuit will replace the current cooling system, which will be simply bypassed. The current cooling system uses a plate heat exchanger with water as the cooling fluid, operating in a closed circuit. Transitioning to the new system with R1270 will provide greater efficiency in the cooling process, maintaining the desired temperatures and improving the overall energy efficiency of the plant.

4.8 Factory Acceptance Test (FAT)

This document outlines the Mechanical Factory Acceptance Test (FAT) protocol and the corresponding report for the MBC unit. The protocol encompasses a series of tests and inspections designed to verify the functionality and proper configuration of the equipment.

The document is organized as follows:

1. Visual Inspection: This section includes a review of the documentation, measurement of overall dimensions, and inspection of equipment such as valves, pressure devices,

pressure indicators, and other instrumentation. It is crucial to verify the correct operation of the system by checking labelling, wiring, and connections of each component. Additionally, it is essential to ensure that all check valves are correctly positioned and installed according to the direction indicated by the arrow. The proper operation of actuated valves should be confirmed by testing their open/close functionality via the HMI and verifying their actual positions during Emergency Shutdown (ESD) conditions.

2. System Leak Test: A leak test was conducted using nitrogen, with a testing pressure of 1 bar to ensure system integrity.
3. Operational Test: This test aims to demonstrate that the MBC test bench operates safely under the desired conditions. Specific tests were performed on the heat exchangers, furnace, two pumps, the cooler installed for the cooling circuit, and the H_2S, HCl, H_2, and CO_2 detection noses. Additionally, an Emergency Shut Down (ESD) test was conducted by pressing the emergency stop button located on the main control panel to verify proper functionality.

During the Factory Acceptance Test, it was noted that check valves numbered 107 and 109 were physically missing from the test bench. Only check valve CV-107 will be installed, as it is required for operation. An additional check valve has been added above the adsorption column and labelled CV-109 in place of the non-existent valve. Furthermore, a ball valve was added above the sparger, following the PSV, to facilitate fluid isolation or diversion if needed. All these modifications have been documented in the P&ID and the associated instrument lists have been updated accordingly.

During the visual inspection, significant nitrogen leaks were detected along the lines. In order to identify the sources of these leaks, a soap and water solution was used to point areas where soap bubbles formed: ive distinct leak areas were identified, which were localized near valves and filters. Thus, the affected areas were subsequently tightened to solve the issue.

4.8.1 Key Sections of the Factory Acceptance Test (FAT) Document for MBC

The following sections outline the key components of the Factory Acceptance Test (FAT) protocol for the MBC unit. This protocol includes tests and inspections to verify functionality and proper configuration.

Functional Testing with Process Fluids will be conducted upon commissioning of the plant after installation on-site. Operational checks and tests will be performed on-site. Please refer to the "MBC Test Bench Manual" for detailed procedures.

Visual Inspection

The consistency of pre-assembled circuits is verified in the workshop against the P&ID.

1. Documentation Review:
    - Ensure all drawings and documents are current and align with the constructed unit.
2. Equipment Inspection:

- To verify the correct operation of the system, check the labeling, wiring, and connections of each piece of equipment. The following tables list all equipment, instruments, and associated valves.

Tabella 3: Attrezzatura

Tag	Descrizione	Dimensione caratteristica	Check	Commenti
C-101A	Colonna	OD 60 mm, H 1500 mm	✓	
E-101	Cavo Riscaldante	0,6 kW	✓	
E-120	Cavo Riscaldante	30 W/m, 9 mt	✗	Non montato (attualmente non necessario)
E-102	Scambiatore di Calore	2 kW	✓	
E-103	Forno Tubolare	2,7 kW	✓	
E-105	Raffreddatore circuito di raffreddamento	1,5 kW	✓	
FIL-101	Filtro a T	141 µm	✓	
FIL-102	Filtro a T	141 µm	✓	
FIL-103	Filtro a T	141 µm	✓	
FIL-104	Filtro a T	141 µm	✓	
FIL-105	Filtro a T	141 µm	✗	Controllare loop acqua
FIL-106	Filtro a cartuccia	141 µm	✓	
MP-101	Motore Pompa	0,25 kW	✓	
P-101	Pompa	100 l/h @ 16 barg	✓	
MP-102	Motore Pompa	0,37 kW	✓	
P-102	Pompa	200 l/h @ 2 barg	✓	
T-101	Gorgogliatore	DN 150	✓	
T-102	Vessel	DN 50, H 250 mm (0,5 L)	✓	
T-103	Vessel	5 l	✓	

- Check Valves:
  - Ensure all check valves are correctly positioned and installed according to the direction indicated by the arrow.

Tabella 4: valvole di controllo

Tag	Tipologia	DN	Check	Commenti
CV-101	Check	12 mm	✓	
CV-102	Check	12 mm	✓	
CV-103	Check	12 mm	✓	
CV-104	Check	12 mm	✓	
CV-105	Check	12 mm	✓	
CV-106	Check	12 mm	✓	
CV-107	Check	12 mm	✗	Da montare
CV-108	Check	12 mm	✓	
CV-109	Check	12 mm	✓	Utilizzata come PSV

- Actuated Valves:
  - Verify the correct opening and closing of actuated valves using the HMI. Check the actual position against the Emergency Shutdown (ESD) status.

Tabella 8: Valvole attuate

Tag	Check HMI	Posizione ESD	Commenti
YV-120	Da fare	NC	
YV-101		NC	
YV-102		NC	
YV-103		NC	
YV-104		NC	
YV-105		NC	
YV-106		NC	
YV-107		NC	
YV-108		NC	
YV-109		NC	
YV-110		NC	
YV-111	Da fare	NC	
YV-115	Da fare	NC	

- Actuated Valves:

Tabella 5: Valvole manuali

Tag	Tipologia	Posizione	Check	Commenti
BV-101	Sfera		✓	
BV-101A	Sfera		✓	
BV-101B	Sfera		✓	
BV-102	Sfera		✓	
BV-103	Sfera		✓	
BV-104	Sfera		✓	
BV-105	Sfera		✓	
BV-106A/B	Sfera		✓	
BV-107	Sfera		✓	Controllare modello
BV-108	Sfera		✓	Aggiungere tag
NV-101	Spillo		✓	
NV-102	Spillo		✓	
NV-103	Spillo		✓	

- Other instruments:

Tag	Descrizione	Da	A	Unità	Check	Commenti
AT-101/102	Sensore di concentrazione HCl/H2S	0	100	ppm		
AT-103	Sensore ambientale HCl	0	100	ppm		
AT-104	Sensore ambientale H2S	0	100	ppm		
AT-105	Sensore ambientale CO2	0	100	ppm		
AT-106	Sensore ambientale H2	0	100	ppm		
DPT-101	Sensore Dew-Point in ingresso	-100	20	°C	-	Non funzionante
DPT-102	Sensore Dew-Point in uscita	-100	20	°C	-	Non funzionante
LT-101	Misuratore di livello T-101	-	-	-	-	Fare zero
LSH-202	Livellostato T-102	-	-	-	-	Da montare*
PI-102	Manometro uscita C-101	0	16	barg		
PI-105	Manometro uscita P-101	0	25	barg		
PT-101	Sensore di pressione in ingresso	0	16	barg		
PT-104	Sensore di pressione in uscita	0	16	barg		
TT-101	Sensore di temperatura in ingresso	0	200	°C		
TT-102A/B/C	Sensore di temperatura T-101	0	200	°C		
TT-103A/B	Sensore di temperatura C-101	0	200	°C		

Tag	Descrizione	Da	A	Unità	Check	Commenti
TT-103C	Sensore di temperatura per C-101	0	1000	°C		
TT-104	Sensore di temperatura per E-102	0	200	°C		
TT-205	Sensore di temperatura per E-105	0	200	°C		
FCV-101A	Regolatore di portata CO2 - bypass	0	21	barg		
FCV-101B	Regolatore di portata CO2	0,02	1	Nm3/h		
FCV-102	Regolatore di portata N2	0,05	2,5	Nm3/h		
FCV-103	Regolatore di portata N2+H2S+HCl	0	0,1	Nm3/h		
FCV-104	Regolatore di portata H2	0,08	4	Nm3/h		
PCV-201	Regolatore di portata uscita	0	21	Nm3/h		

3. System Leak Test:
    - The leak test will be conducted using nitrogen with a test pressure of 1 bar. Specific lines have been selected to identify lea. Five leak areas were identified and have been addressed accordingly.
4. Operational Test:
    - The operational test is intended to demonstrate that the MBC unit can operate safely under the desired conditions.
    - Tests:
        - 4.1) Heat Exchanger E-101
        - 4.2) Heat Exchanger E-102
        - 4.3) Furnace E-103
        - 4.4) Pump P-101
        - 4.5) Pump P-102
        - 4.6) Cooling Circuit Cooler E-105
        - 4.7) Sensor ATI-101
        - 4.8) Sensor ATI-103
        - 4.9) Sensor ATI-104
        - 4.10) Sensor ATI-105
        - 4.11) Sensor ATI-106

- 4.12) Emergency Shutdown Test
  - Press the emergency stop button on the main panel and verify that all systems function correctly.
  - Tested, procedure functioning.

5. HMI Interface:
   - Visualization of graphical pages.
   - Tested, procedure functioning.

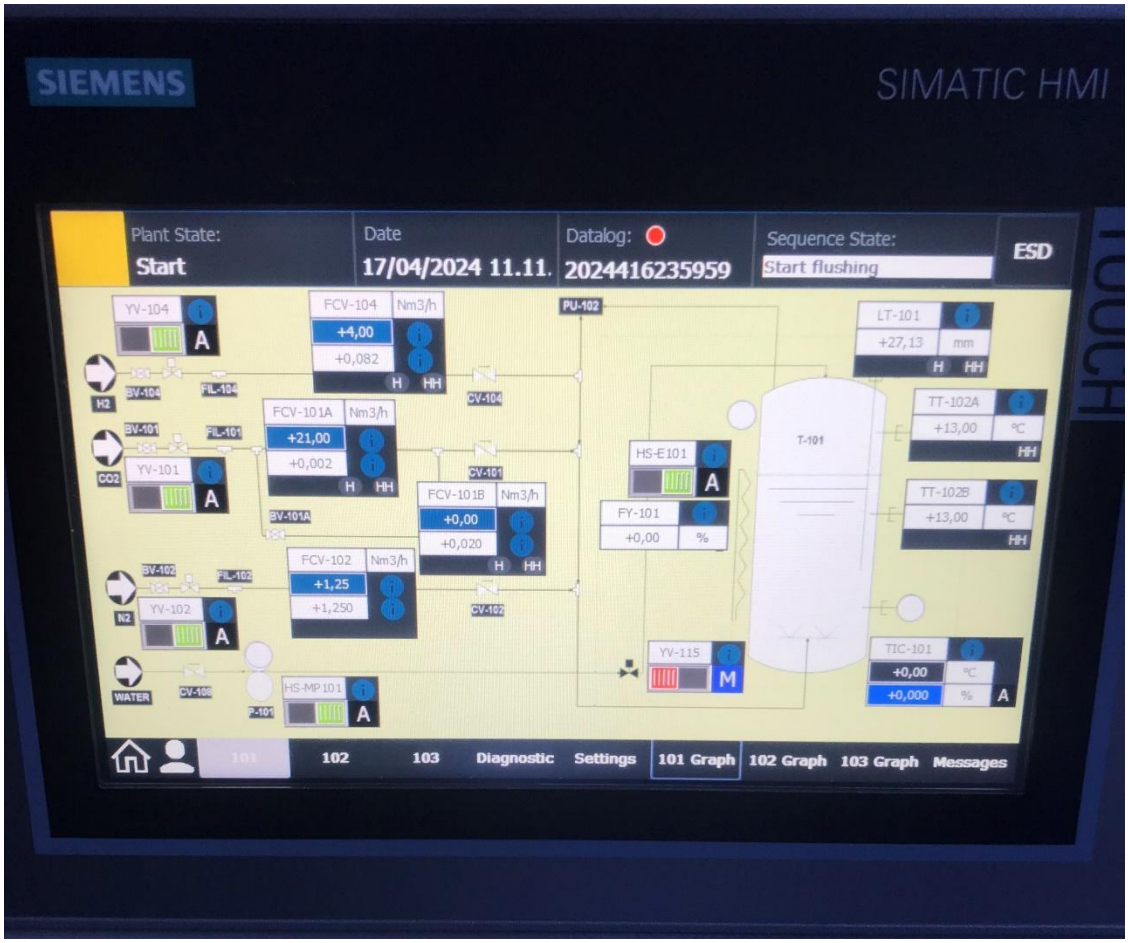

Figure 15. Loop 101

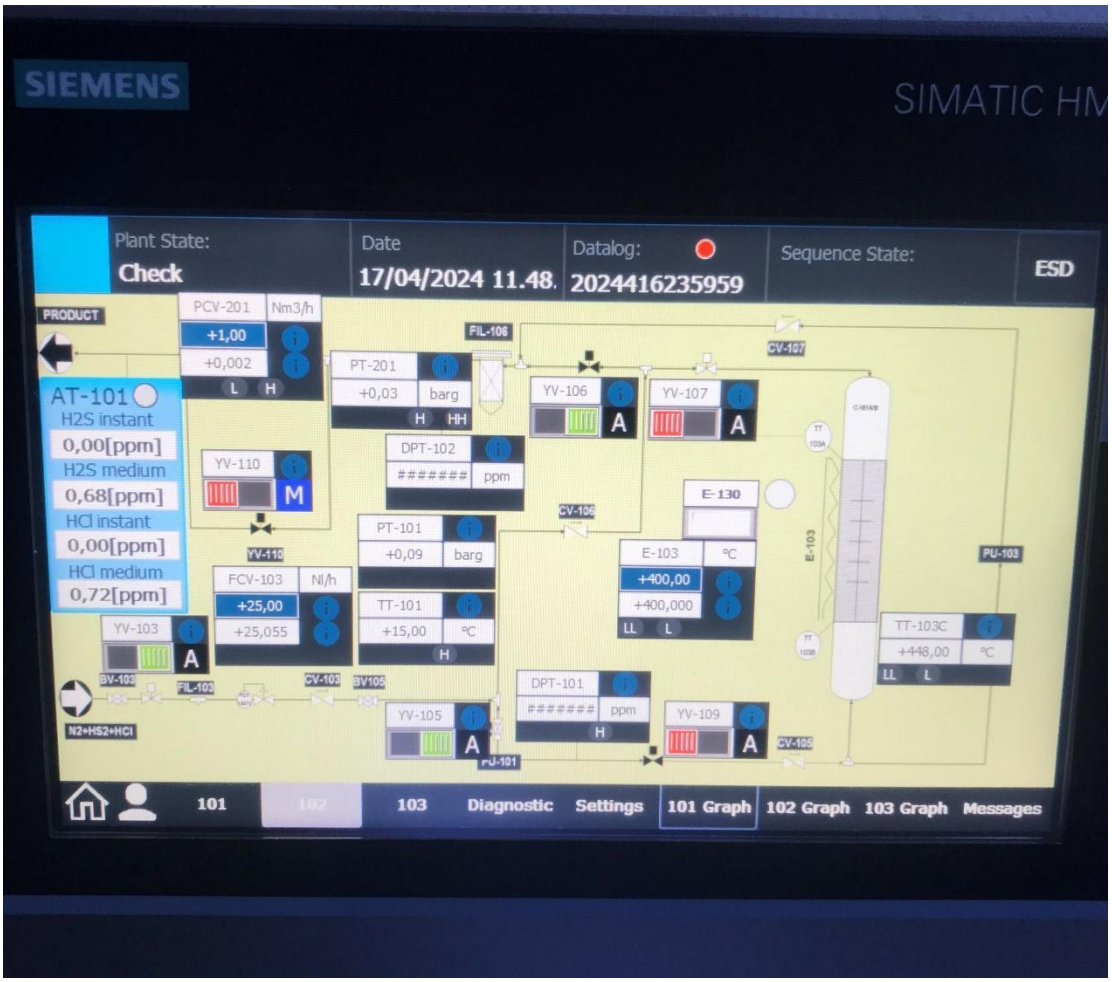

Figura 16. Loop 102

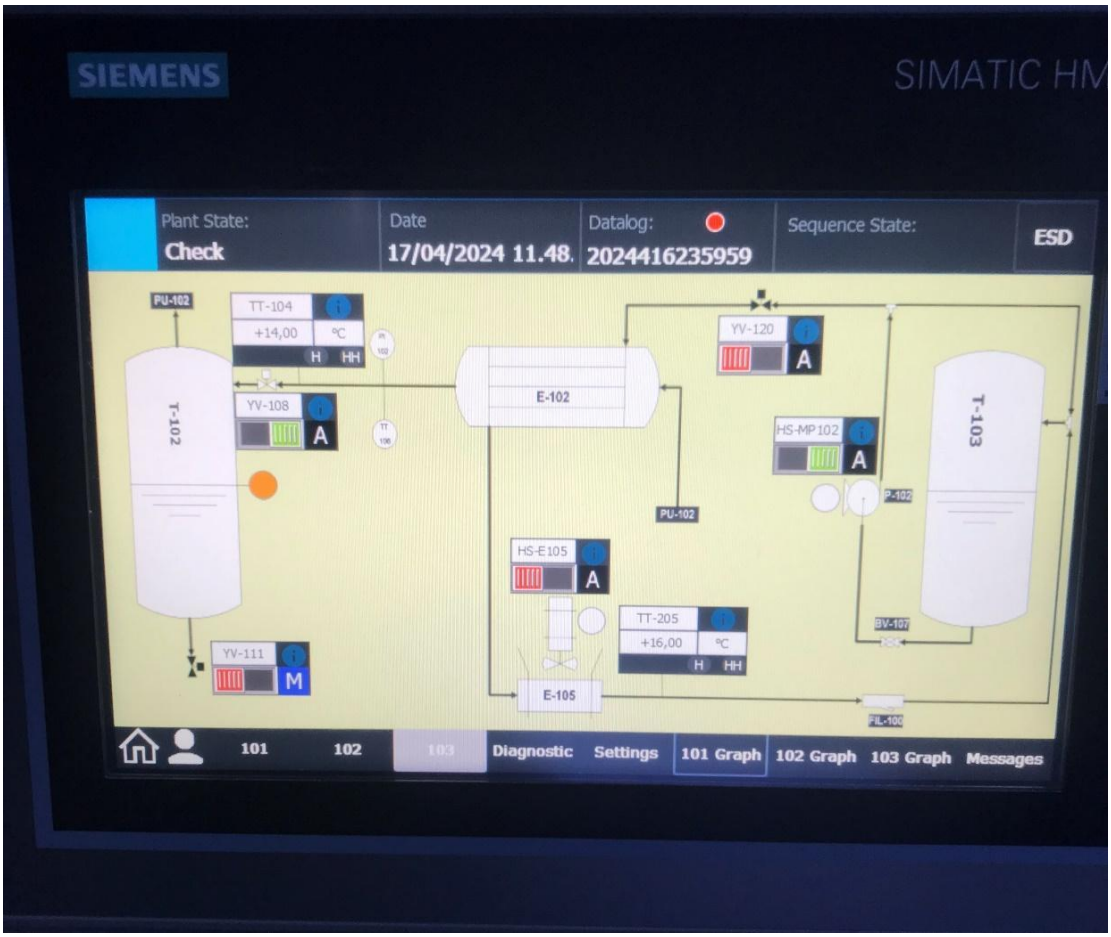

Figura 17. Loop 103

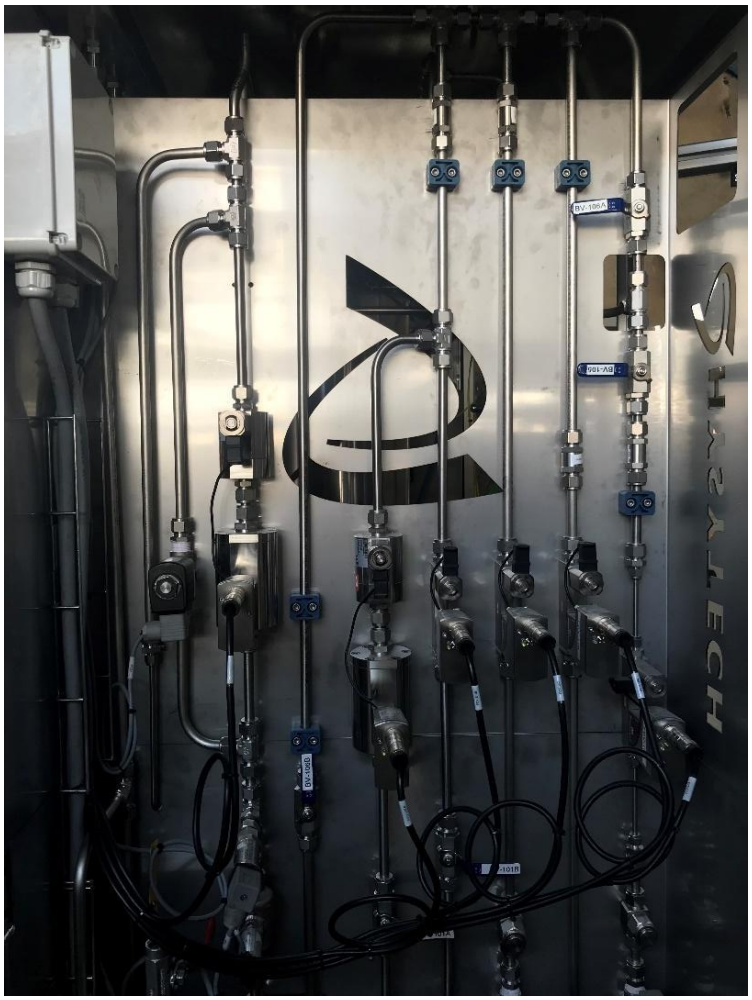

Figura 18. Inlet fluids and a portion of the cooling loop

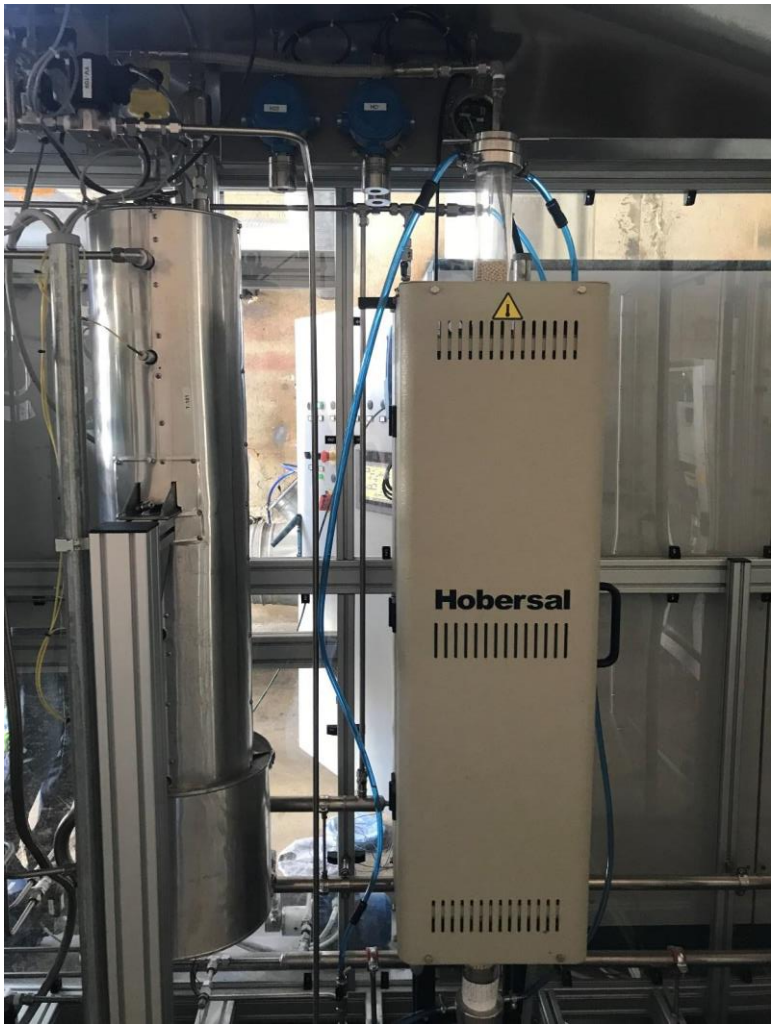

Figura 19. Heat exchanger E-103 and adsorption column C-101A

Figura 20. E-105

4.8.2 Mass Flow Controller

In the context of gas flow measurement, accurate calibration of mass flow controllers (MFCs) is crucial to ensure precise operation in various applications. This section addresses the process of recalibrating the FCV-101A, initially set for methane (CH_4), for use with carbon dioxide (CO_2). The aim is to determine the appropriate conversion factor to adjust the flow readings for CO_2, given that the original calibration is based on methane. The FCV-101A was originally calibrated for methane, but due to the need to measure CO_2 flows, a conversion factor must be determined. This factor adjusts the readings from the mass flow controller (MFC) to accurately reflect the flow rate of CO_2 instead of methane.

The testing involved a low-pressure dry-base test using a mixture of gases: nitrogen (N_2), carbon dioxide (CO_2), and hydrogen (H_2), with respective volumetric percentages of 58.47%, 29.87%, and 11.66%. Additionally, the test included a concentration of 100 ppm of H_2S/HCl. The flow rates for each component were calculated in normal liters per hour (Nl/h) as follows:

$$\dot{V}_{MFC} = \dot{V}_{tot} \cdot \%vol$$

$$\dot{V}_{MFC,N_2} = 1{,}25\ \frac{Nm^3}{h} \cdot 1000 \frac{Nl}{Nm^3} \cdot 58{,}47\ \% = 730{,}88 \frac{Nl}{h}$$

$$\dot{V}_{MFC,CO_2} = 1{,}25\ \frac{Nm^3}{h} \cdot 1000 \frac{Nl}{Nm^3} \cdot 29{,}87\ \% = 145{,}75 \frac{Nl}{h}$$

$$\dot{V}_{MFC,H_2} = 1{,}25\ \frac{Nm^3}{h} \cdot 1000 \frac{Nl}{Nm^3} \cdot 11{,}66\ \% = 373{,}38 \frac{Nl}{h}$$

HCl/H2S component is expressed as 0,01% vol, thus:

$$\dot{V}_{MFC,HCl} = 1{,}25\ \frac{Nm^3}{h} \cdot 1000 \frac{Nl}{Nm^3} \cdot 0{,}01\ \% = 12{,}5 \frac{Nl}{h}$$

The full scale, which is the flow rate value indicated on the nameplate of each FCV for the specific gas, and the range indicator used for the gases in the MFCs, is shown in the table below. A percentage comparison between the full-scale values and those of the mass flow controllers will be useful later.

Gas	**Fondo Scala**	**UOM**
N_2	25	Nm^3/h
H_2	20	Nm^3/h
CO_2	0,1	Nm^3/h
CH_4	21	Nm^3/h

In this case, the FCV-101A has been calibrated for methane, but we intend to use it for a in the attached Piping and Instrumentation Diagram (P&ID), we observe a detailed process flow

system that is likely part of an industrial gas or liquid processing unit. It also contains key elements essential for the control and operation of a complex process system, including vessels, heat exchangers, control valves, and instrumentation that ensure safe and efficient operations. I will provide a short overview and highlight important aspects based on a general analysis of the diagram.

The process flow begins at the top left, where fluid enters through a feed stream, passing through several valves and instrumentation before reaching the heat exchanger. This system contains multiple inline instruments, such as flow transmitters (FT), pressure transmitters (PT), and level transmitters (LT), each designed to measure and transmit data related to the fluid's properties such as flow rate, pressure, and level. Furthermore, there is considerable instrumentation represented across the system, which indicates a high level of automation and control. The control loops include Pressure Control Loops, which maintain system pressure within specified limits, likely protecting the equipment from overpressure situations; flow control loops, that ensure the process fluid moves at the correct rate to maintain system efficiency; level control loops, particularly around the vessel, these loops ensure that the liquid level in the vessel is maintained to avoid overflows or dry runs.

All these control systems are also tied to alarms and emergency shutdown systems, ensuring safe operation under all conditions.

flow. Therefore, it will be necessary to determine the so-called conversion factor to obtain the full-scale value for the gas that will actually be flowing through the device. The table below provides the necessary data for these calculations.

	Gas 1	Gas 2
Name	**Methane**	**Carbon Dioxide**
Cp (cal/gK)	0,568	0,213
ρ (g/l)	0,7175	1,977

The conversion factor C can be assessed by the ratio:

$$C = \frac{c_{p1} \cdot \rho_1}{c_{p2} \cdot \rho_2}$$

In which:

c_p is the specific heat

ρ is the density at normal conditions

(1) Gas calibrated
(2) Gas to be measured

In this way we obtain a conversion factor of 0,968. Once obtained this, we can now calculate the full-scale value of every FCV, in particular the one we need the conversion, where:

$$FS_{CO_2} = C \cdot FS_{CH_4}$$

FCV	From	To	C	FS [Nm^3/h]
102	N_2	N_2	1	25
103	N_2	N_2	1	25
104	H_2	H_2	1	20
101A	CH_4	CO_2	0,968	20,32
101B	CO_2	CO_2	1	0,1

The comparison between the full-scale values and the ones of the MFC will be:

$$\frac{\dot{V}_{MFC}\left(\frac{Nl}{h}\right)}{\dot{V}_{FS}\left(\frac{Nm^3}{h}\right)\cdot 1000\frac{Nl}{Nm^3}}$$

In this way we obtain:

29,2% for N_2

9,3% for H_2

14,6% for CO_2

12,5% for H_2S/HCl

4.9 User Manual and Operation of the MBC Test Bench

I have been requested to draft a manual concerning the operation and use of the MBC test bench, specifically addressing both dry and wet analysis procedures.

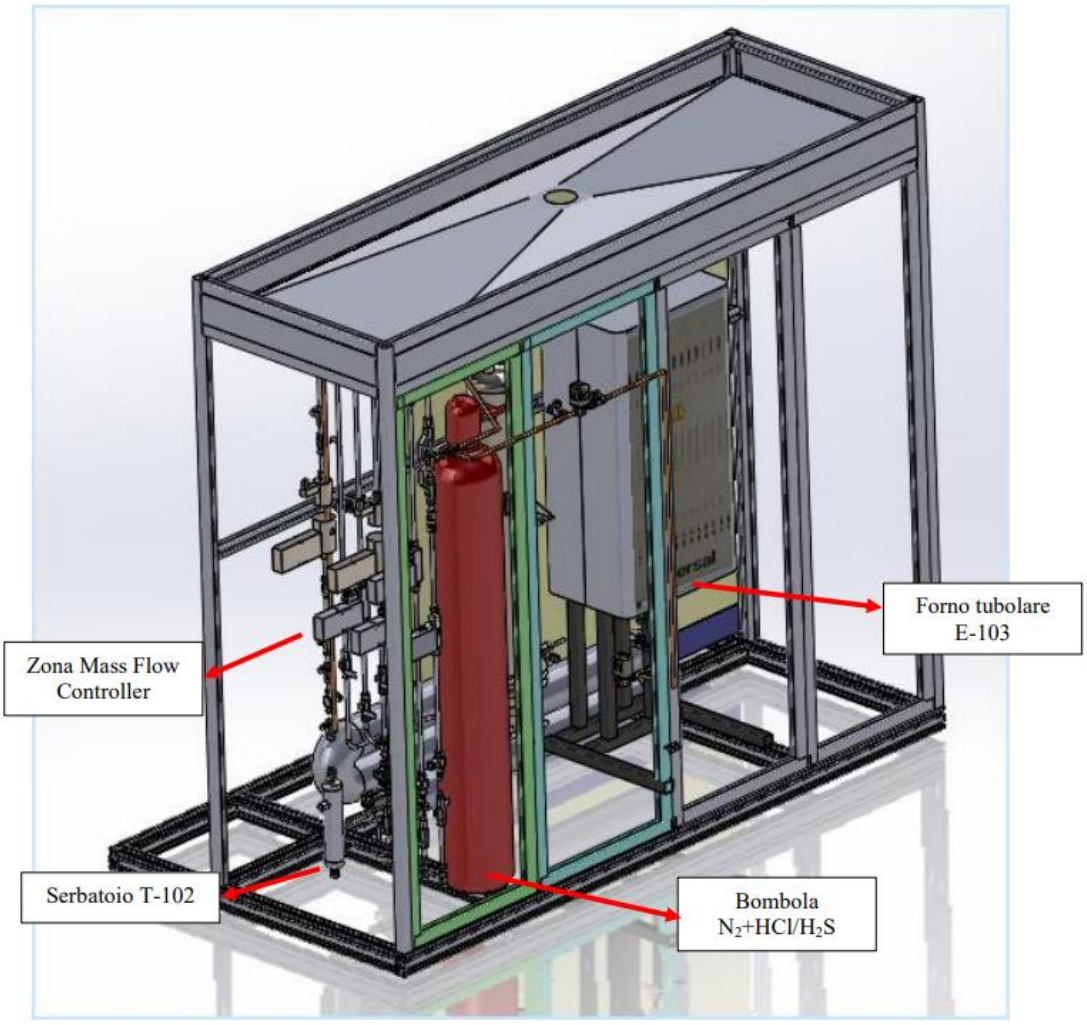

Figure 21a. Bench scheme (created by DWG unit in Hysytech)

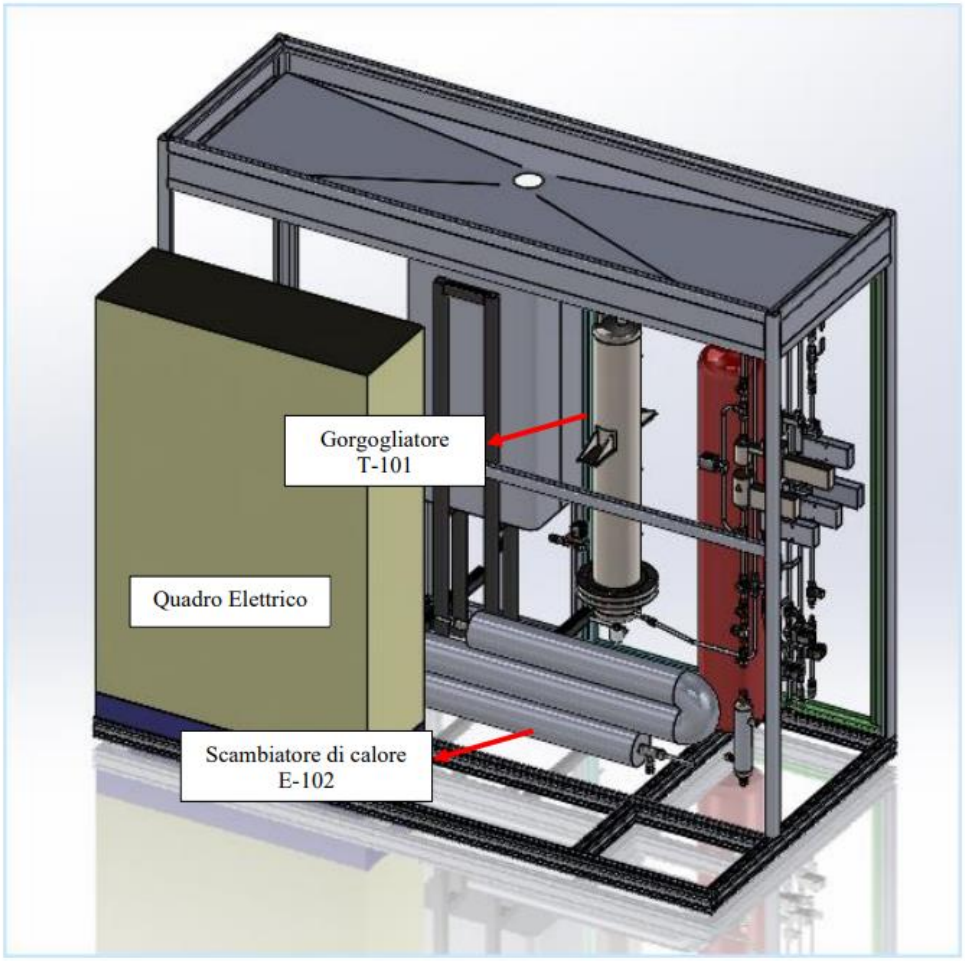

Figure 21b. Bench scheme (created by DWG unit in Hysytech)

Dry Analysis – Dry Test

Procedure for Conducting an Analysis Without Water

1. Gas Sampling:
   - Sample the following gases from their respective cylinders using valves RV-103, RV-104, RV-101, and RV-102:
     - N_2+H_2S+HCl
     - H_2
     - CO_2
     - N_2
2. Manual Valve Operation:
   - Manually open the ball valves BV-103, BV-104, BV-101, and BV-102.
   - For the CO_2 flow, open valve BV-101B and close BV-101A, as the latter is dedicated to bypass.
3. Activation of Shut-Off Valves:
   - Activate the shut-off valves via the HMI: YV-103, YV-104, YV-101, and YV-102.
4. Furnace Temperature Adjustment:
   - Activate furnace E-103 via the HMI and set it to 400°C. Wait until the process temperature matches the set point.
5. Setting Gas Flow Rates:

- Input the desired flow rates in Nm^3/h via the HMI for FCV-104, FCV-101A, FCV-101B (set to 0 as indicated in point 3), and FCV-102. Verify that the indicated flow rates are achieved by monitoring the process values shown below.

6. Measurement of Components:
   - To measure the initial amounts of H_2S and HCl, direct the flow straight to the analyzer, bypassing the adsorption column. Open ball valve BV-106A and close BV-106B. Ensure that shut-off valves YV-105 and YV-107 are closed, and YV-106 is open.
   - To allow the flow through the adsorption column, open YV-107 and close YV-106.

Analysis with Water – Wet Test

Procedure for Conducting an Analysis with Water

1. Gas and Water Sampling:
   - Sample the gases from their respective cylinders using valves RV-103, RV-104, RV-101, and RV-102 as described in the previous section.
   - Sample water from the cylinder to feed the tank T-103.
2. Manual Valve Operation:
   - Manually open the ball valves BV-103, BV-104, BV-101, and BV-102.
   - For the CO_2 flow, open valve BV-101B and close BV-101A, which is dedicated to bypass.
   - Open valve BV-106B to direct the mixture to the sparger.
3. Activation of Shut-Off Valves:
   - Activate the shut-off valves via the HMI: YV-103, YV-104, YV-101, and YV-102.
4. Furnace Temperature Adjustment:
   - Activate furnace E-103 via the HMI and set it to 400°C. Wait until the process temperature reaches the set point.
5. Setting Gas Flow Rates:
   - Input the desired flow rates in Nm^3/h via the HMI for the FCVs. Verify that the indicated flow rates are achieved by monitoring the process values below.
6. Pump Activation and Water Level Monitoring:
   - Activate pump P-101 via the HMI to supply water to the sparger.
   - Ensure that there is always an adequate water level in tank T-103 by observing the level indicator next to the tank.

4.10 MATLAB Code Implementation

The MATLAB code for the theoretical model was developed by the previous thesis student who initiated this project last year:

```
clc
clear all
%close all

%% Parameters
De = 7.84e-6; % De [m2/s] --> ZnO
rho_b = 1.9e3; % Solid density [kg/m3] --> METTERE DENSITÃ  ZnO
Dp = 6; % Particle diameter [mm] --> METTERE DIAMETRO ZnO (diametro equivalente)
Rp = Dp/2; % Particle radius [mm]
b=1; % Reaction Stoichiometry
M_b=81.38; % ZnO MW [kg/kmol]
tau=0.4; % Residence time [s]
V=1.55/3600; % Volumetric Flow rate [m3/s]
D=0.057; % Column Diameter [m]
M=0.3; % usage factor of ZnO
H=0.04; % Column Height [m]
% C_ppm=30; % ppm Concentration
C_ppm=70; %H2S
C_a0 = C_ppm*1.81e-8; % Initial HCl concentration [kmol/m3]
n=round(H/(Dp/1000)); % #part (calcolato come H/Dp)
r_0(1:n,1)=Rp-0.1*Rp; % Initial core radius [m] (per evitare -Inf)
input_par=[De, rho_b,Dp,Rp,b,M_b,V,D,H,C_a0,n,M]; % vettore con parametri necessari
alle funzioni successive
%tspan = [0 6*3600]; % Time interval
tspan = [0,140]; % Time [h]

%% ODE system

%options=odeset('OutputFcn',@OutputFcn);
[t,y] = ode15s(@(t,y)drdt1(t,y,input_par),tspan,r_0); % funzione che restituisce i
tempi t e i risultati y, che rappresentano...
                                                    ... l'evoluzione del raggio delle
particelle nel tempo


% Solve ODE system_OLD
%
% C_a=zeros(length(t),1);
%  for i=1:length(t)
% dNa_dt=-4*pi*D*C_a0/(1/r_s(i)-1/R);
% C_a(i)=C_a0-dNadt(i);
% alpha=b*D*C_a(i)*M_b/(rho_b);
% dr_dt = @(t, y) -alpha/(y-y^2/R);
% [t,r] = ode15s(dr_dt, tspan, r_0);
% end

%% Evaluating Ca
% calcola la concentrazione di H2S lungo il reattore e determina il tempo
% di BT
r_s=y;
t=t;
Ca(length(t),n)=zeros;
Ca(:,1)=C_a0;
N=round(D^2/4/(Rp/1000)^2); % #part per sezione (calcolato come S/Sp)
delta=(4*pi*De*N/V)/1000;
```

```
gamma=b*De*3600*1e6*M_b/(rho_b*M)*C_a0; % drdt=-gamma*Ca/(r-r^2/R)


for i=2:n
    for k=1:length(t)
        Ca(k,i)=Ca(k,i-1)*(1-delta/(1/r_s(k,i-1)-1/Rp));
%         if Ca(k,i)<0
%             Ca(k,i)=0;
%         end
    end
end

% BT time evaluation

tBT=zeros(1,n);
for i=1:n
    for k=1:length(t)
        if Ca(k,i)>0.01*C_a0
            BT=t(k);
            break
        end
        tBT(i)=BT;
    end
end

TBT=zeros(1,5);
%TBT(1)=(tBT(:,10));
TBT(2)=(tBT(:,round(n/4)));
TBT(3)=(tBT(:,round(n/2)));
TBT(4)=(tBT(:,round(3*n/4)));
TBT(5)=(tBT(:,end));

Ca=Ca/1.81e-8;
results=[t,Ca(:,end)];
CBT=zeros(length(t),1);
CBT(:,:)=1;

%% Plot
figure
% plot BT curves at different bed heights (as sorbent layers)
plot(t,Ca(:,end),t,CBT,t,Ca(:,round(n/4)),t,Ca(:,round(n/2)),t,Ca(:,round(3/4*n)),t,Ca(
:,end),LineWidth=2)
xlabel('time [h]');
ylabel('Ca_H_2_S [ppm]');
title(['Break-Through Curves [H = ',num2str(H),' m]']);
legend('BT-Curve','CBT','z/4','z/2','3z/4');

%% ODE FUNCTION
function drdt = drdt1(t,y,input_par)

% input_par={De, rho_b,Dp,Rp,b,M_b,V,D,H,C_a0,n,r_0,M}; definisco ogni
% parametro in base alla posizione nel vettore
 De=input_par(1); % De [m2/s]
 rho_b=input_par(2); % Solid density [g/m3]
 Dp=input_par(3); % Particle diameter [mm]
 Rp=input_par(4); % Particle radius [m]
 b=input_par(5); % Reaction Stoichiometry
 M_b=input_par(6); % K2CO3 MW [g/mol]
 V=input_par(7); % Volumetric Flow rate [m3/s]
 D=input_par(8); % Column Diameter [m]
 H=input_par(9); % Column Height [m]
```

```
 C_a0=input_par(10); % Initial HCl concentration [mol/m3]
 n=input_par(11);
 M=input_par(12);
drdt=zeros(n,1);
Caf(1:n,100)=zeros;
Caf(1,:)=1;
gamma=b*De*3600*1e6*M_b/(rho_b*M)*C_a0; % drdt=-gamma*Ca/(r-r^2/R)
N=round(D^2/4/(Rp/1000)^2); % #part per sezione (calcolato come S/Sp)
% M=0.2; % mass fraction of K2CO3
delta=(4*pi*De*N/V)/1000;

drdt(1) = -Caf(1)*gamma/(y(1)-y(1)^2/Rp);

if y(1)<1e-5
    drdt(1)=0;
    y(1)=0;
end
  for i=2:n
    Caf(i)=Caf(i-1)*(1-delta/(1/y(i-1)-1/Rp)); % MB(equation)
    %Caf(i)=Caf(i-1)+(rho_b/M_b*4*pi*y(i-1)^2*drdt(i-1))*N/V; % MB(derivative form)
% if Caf(i)>0
%     Caf(i)=Caf(i);
% else Caf(i)=0;
%end
% if Ca(i)<C_a0
%     Ca(i)=Ca(i);
% else Ca(i)=C_a0;
%end
     drdt(i) = -Caf(i)*gamma/(y(i)-y(i)^2/Rp); % SCM equation
     if y(i)<1e-5
         drdt(i)=0;
         y(i-1)=0;
     end
  end
end
```

The MATLAB code presented constitutes a numerical model for simulating the adsorption process of H_2S on ZnO in a fixed-bed reactor. In the initial phase, the parameters describing the properties of the system and particles are defined. Subsequently, a system of ordinary differential equations (ODE) is implemented to describe the temporal evolution of the particle radius in the reactor bed. This system is represented by the function drdt1.

To solve the ODEs, the function ode15s is employed, which is suitable for solving stiff and non-stiff systems. The solution occurs over a time interval defined by the vector tspan, representing the period during which the process is simulated.

Next, the concentration of H_2S along the reactor is calculated based on the chosen adsorption model, using the initial concentrations and particle radius as input. Additionally, the breakthrough time (BT), defined as the time required for the H_2S concentration at the reactor outlet to reach a certain threshold, is evaluated. Finally, a plot is generated showing the breakthrough curves for various bed heights of the reactor, along with the H_2S concentration at the outlet and the breakthrough concentration (CBT).

Focusing on specific parts of the code, the following can be observed:

- The function ‘drdt1’ represents the differential equations that describe the evolution of the particle radius, based on the mass transport and adsorption model. The reaction rate ‘drdt’ for each particle in the reactor bed depends on the adsorbed H_2S concentration, defined by the matrix ‘Caf’, and the particle radius y. An if loop is implemented to ensure that if the particle radius becomes too small, the reaction rate is set to zero to avoid non-physical values.
- The function ‘ode15s’, a numerical method for solving ODEs, is used to address the stiff system of differential equations.
- The BT time is evaluated for different bed heights to understand the time required for the adsorbent material to become fully saturated.

It is important to note that the breakthrough concentration was defined as 1% of the initial concentration. Generally, the CBT is arbitrarily defined depending on the adsorption applications. In this case, it was considered that fuel cells can withstand up to 1 ppm of H_2S and HCl. As a precaution, an initial concentration of 70 ppm was chosen instead of 100 ppm, in order to have a CBT of 0.7 ppmv with a margin of 0.3 ppmv. Therefore, through an ‘if’ loop, it was imposed that when the concentration exceeds 1% of the initial H_2S concentration, the corresponding time is recorded as the breakthrough time for that particle. The final result is a vector tBT that contains the breakthrough times for each particle in the reactor bed.

The following figures demonstrate that each test lasts less than 9 hours, utilizing a 4 cm bed (with the remainder consisting of inert material) and 150 ppm of H2S.

By means of the MATLAB model, the objective is to achieve 70 ppm of H2S with a nitrogen flow rate of 1.25 Nm^3/h. Given that the analyser can read a maximum value of 100 ppm, it is necessary to determine an appropriate combination of mass flow rate and test duration to ensure that the test duration does not exceed 17 hours. This goal can be accomplished, for instance, by using a flow rate of 1.4 Nm^3/h and an initial H2S concentration of 70 ppm. Under these conditions, each test should last approximately 16 hours, as illustrated

Since a steeper profile with an S-shaped curve is required, various configurations were analyzed by using a constant mass flow rate for different concentration values, ranging from 70 to 90 ppm, considering that the analyzer can read up to a maximum of 100 ppm. This analysis was conducted for different mass flow rates, from 1.25 Nm^3/h to 1.55 Nm^3/h. At higher values, the results would be unacceptable because the breakthrough concentration (CBT) would exceed the breakthrough (BT) curve. Below, all the case studies are presented, categorized by each mass flow rate value.

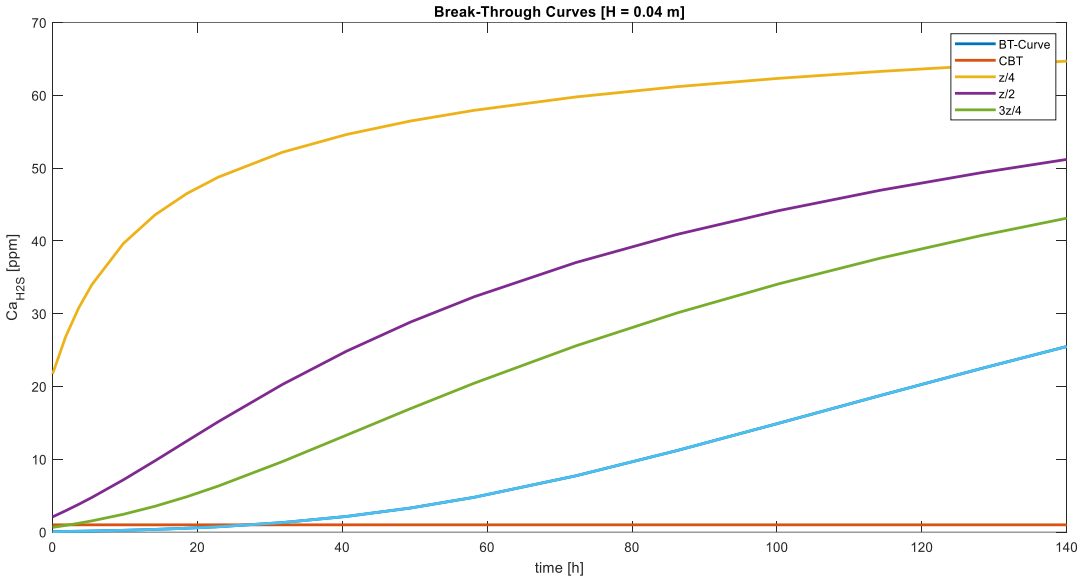

Graph a. 1.25 Nm3/h, 70 ppm

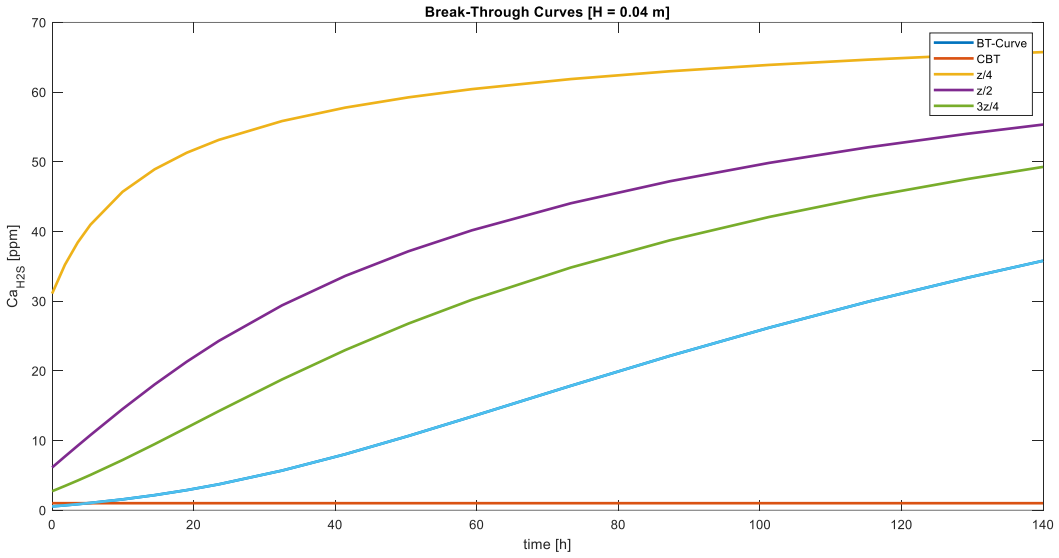

Graph b. 1.25 Nm3/h, 80 ppm

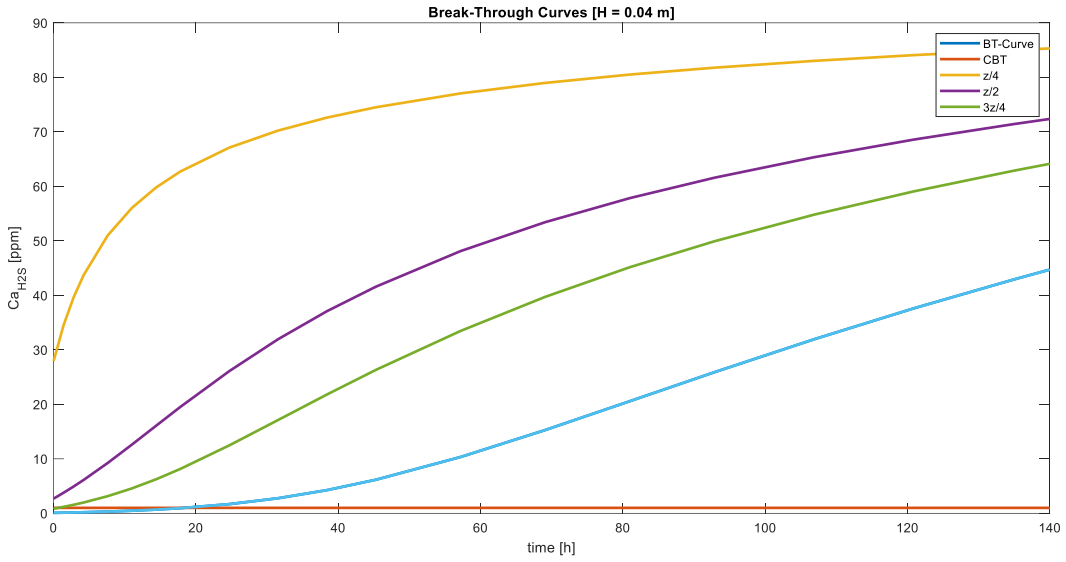

Graph c. 1,55 Nm3/h, 70 ppm

It seemed that the best choice is the one at 70 ppm, with 1,55 Nm3/h of nitrogen mass flow rate, ensuring the non-overwhelming of the system: a nitrogen mass flow rate of 1.55 Nm^3/h, combined with 70 ppm, produces a steeper S-shaped breakthrough curve, making the profile more preferrable as it indicates a more abrupt transition between the adsorption phase and the breakthrough point, which allows for a clearer determination of the breakthrough time (BT) and breakthrough concentration (CBT). At this flow rate and concentration, the test duration is optimized to be around 16 hours, which is ideal for conducting thorough and precise measurements without exceeding practical testing time constraints, such as the 17-hour limit. It balances the need for detailed data collection with the operational feasibility of the test. Furthermore, the chosen configuration maximizes the efficiency of the adsorption process.

4.10.1 D-optimal design

The D-optimal design is a statistical concept used in experimental design, specifically in situations where the goal is to maximize the efficiency of an experiment with a limited number of trials or resources. It is a type of "optimal design" that seeks to extract the maximum amount of information from an experiment while minimizing the errors associated with parameter estimates.

When designing an experiment, for example, in the fields of chemistry, biology, or engineering, the goal is to understand how input variables (experimental factors) influence an output (response or result). In many cases, performing a full experiment on all possible combinations of variables can be too expensive or inefficient. To address this problem, an optimized sampling strategy, such as the D-optimal design, is used. The D-optimal design is based on a mathematical criterion that seeks to minimize the correlation between the estimated parameters. This is achieved by maximizing the determinant of the Fisher information matrix (or

the X'X matrix, where X is the model matrix), which represents the information gathered from the experiment. The larger the determinant, the better the separability of the estimated parameters. Thus, the D-optimal design selects a set of experimental points (combinations of variable levels) in such a way that the precision with which the parameters of interest can be estimated is maximized, reducing the correlation between them.

Advantages:

- Efficiency: A D-optimal design allows reducing the number of trials needed compared to a full design, while maintaining high-quality parameter estimates.
- Flexibility: It can be used in situations where a classic full factorial design is not feasible due to practical constraints (time, cost, resources).

The Chemometric Agile Tool (CAT) is an advanced software tool used in experimental design, particularly in fields like chemistry and process optimization. It supports the implementation of D-optimal designs, which are crucial in minimizing the number of experiments while maximizing the information obtained from them. In this case, we already have a theoretical model and experimental data, and the purpose is to evaluate their agreement. This can be seen as an application of model validation, where the goal is to determine how well the theoretical predictions fit the experimental observations. One of the key tools for comparing models and data in chemometrics is residual analysis. The residual is the difference between the theoretical value and the experimental value at each point in time:

$$Residual = y_{exp}(t_i) - f(t_i)$$

Where $y_{exp}(t_i)$ is the experimental concentration of H_2S at time (t_i), and $f(t_i)$ is the theoretical prediction at the same time point. By calculating the residuals for each time point, you can assess how closely the model predicts the experimental outcomes.

The CAT method would typically involve several metrics to compare theoretical and experimental trends:

- Sum of Squared Residuals (SSR): This metric sums the squares of the differences between experimental data and model predictions, providing a measure of overall fit:

$$SSR = \sum_{i=1}^{n} (y_{exp}(t_i) - f(t_i))^2$$

  A lower SSR indicates that the theoretical model closely matches the experimental results.

Metrics to compare the theoretical model and experimental data:

- Root Mean Square Error (RMSE): RMSE provides an average error magnitude and is a commonly used metric to quantify the difference between the predicted and observed values:

$$RMSE = \sqrt{\frac{1}{n}\sum_{i=1}^{n}(y_{exp}(t_i) - f(t_i))^2}$$

RMSE is easy to interpret since it is expressed in the same units as the measured quantity (ppm of H_2S), allowing for an intuitive understanding of the error magnitude.

In my analysis, I used the *interp1* function to interpolate the theoretical breakthrough curve at the same time intervals as the experimental data: this allowed for a direct comparison between the two datasets.

This value of RMSE quantifies the difference between the predicted breakthrough curve and the experimental data. To visualize this, I plotted both the experimental data and the theoretical model on the same graph: the experimental data is represented by the blue line, while the breakthrough curve is shown in red; the calculated RMSE is included in the plot's legend for clarity.

The RMSE value was found to be 0.41, giving us an indication of the model's initial accuracy and suggesting that improvements can be made to better align the theoretical predictions with the observed data. The visualization and RMSE calculation are important steps in validating the theoretical model, because by assessing it, we can identify areas where the model may be over- or under-predicting the concentration of H_2S, providing insights into potential adjustments needed to improve its performance.

```
%
interp_BT_curve = interp1(t, Ca(:, end), hours(filtered_timestamps -
filtered_timestamps(1)));
% RMSE
rmse = sqrt(mean((interp_BT_curve - filtered_concentration).^2));

figure;
hold on;

% dati sperimentali
plot(hours(filtered_timestamps - filtered_timestamps(1)), filtered_concentration, 'b-',
'LineWidth', 1, 'DisplayName', 'Dati Sperimentali');

% modello teorico
plot(hours(filtered_timestamps - filtered_timestamps(1)), interp_BT_curve, 'r-',
'LineWidth', 2, 'DisplayName', sprintf('BT-Curve (RMSE = %.2f)', rmse));

% senza ottimizzazione ho un RMSE = 0.41

xlabel('Tempo cumulativo (h)');
```

```
ylabel('Concentrazione H2S (ppm)');
title('Confronto tra BT-Curve e dati sperimentali');
legend('show');
grid on;
```

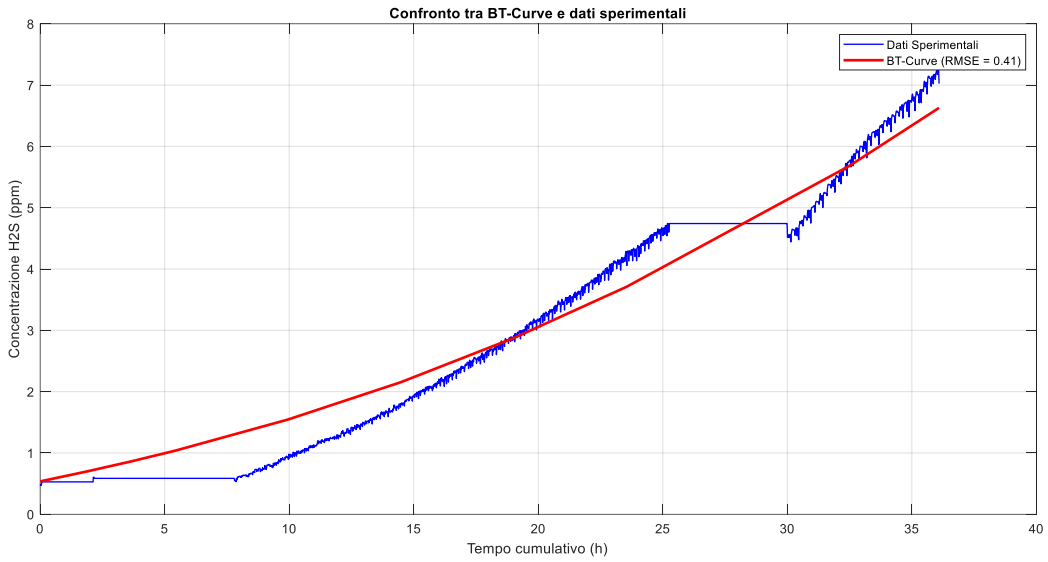

For now, the best option seems to be indeed the configuration with a usage factor of 30%, since with the imposition of values different with respect to this, the RMSE only grows.

- Coefficient of Determination (R^2): indicates how well the theoretical model explains the variance in the experimental data. It is calculated as:

$$R^2 = 1 - \frac{SSR}{Total\ sum\ of\ squares\ (TSS)}$$

where TSS represents the variance of the experimental data from its mean. An R^2 value close to 1 indicates a good fit.

Beyond simple comparison, CAT allows for model robustness analysis. By optimizing the experimental design (e.g., choosing time points or experimental conditions that give the most informative data), CAT helps ensure that the experimental results provide the best possible comparison to the theoretical model.

The MATLAB code for its calculation is showed below.

```
% coefficiente di determinazione (R^2)
ss_res = sum((filtered_concentration - interp_BT_curve).^2);  % somma quadrati dei
residui
ss_tot = sum((filtered_concentration - mean(filtered_concentration)).^2);  % somma
quadrati totali
R2 = 1 - (ss_res / ss_tot);

figure;
hold on;
```

```
% dati sperimentali
plot(hours(filtered_timestamps - filtered_timestamps(1)), filtered_concentration, 'b-',
'LineWidth', 1, 'DisplayName', 'Dati Sperimentali');

% modello teorico
plot(hours(filtered_timestamps - filtered_timestamps(1)), interp_BT_curve, 'r-',
'LineWidth', 2, 'DisplayName', sprintf('BT-Curve (RMSE = %.2f, R^2 = %.2f)', rmse,
R2));

% senza ottimizzazione ho un RMSE = 0.41
% senza ottimizzazione ho un R^2 = 0.95

xlabel('Tempo cumulativo (h)');
ylabel('Concentrazione H2S (ppm)');
title('Confronto tra BT-Curve e dati sperimentali');
legend('show');
grid on;
box on;
hold off;
```

The results guarantee a coefficient of determination of 0.95 for a usage factor of 0.3, thus the approximation made previously by my colleague was very good.

Results

6.1 Empty column test

The empty column test was used as a baseline to establish for the system's behaviour without any sorption or inert material. This test aimed to measure the inherent response time of the system. The test was carried with a 70-ppm concentration of H2S in nitrogen and a total flow rate of 1 Nm3 /h. The test was carried out following the same test procedure and the oven turned off. The response chart is reported in Figure N. The composition of H2S takes 1 to 2 minutes to return to the initial value. Considering that the sorption tests will last for minimum 50 h, the phenomena observed can be neglected.

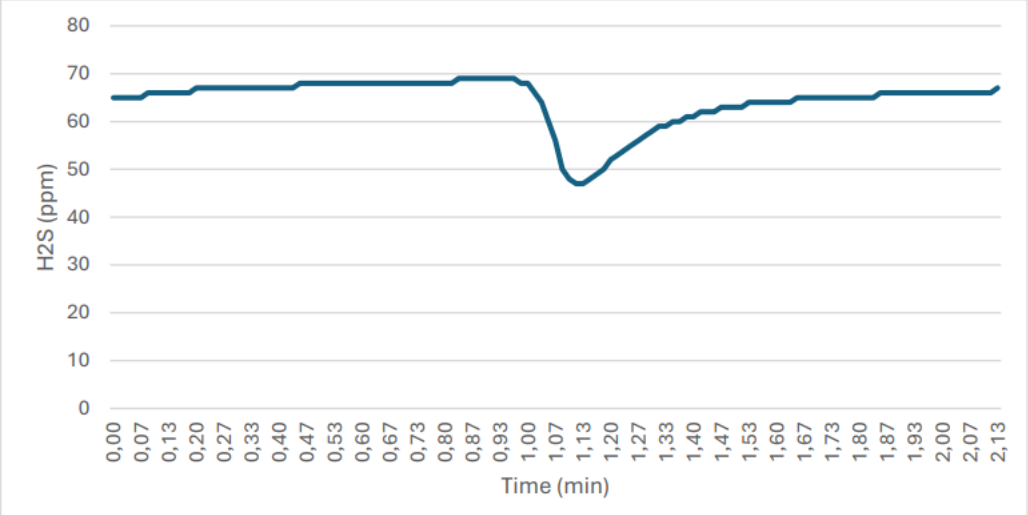

Figure 22. Empty column responses

In this case, the adsorption column was emptied of the inert material and the bed. Initially, I started the sequence normally with the composition check, and after a couple of cycles—alternating between "H2S analysis/pause analysis/washing"—I initiated the Production

sequence, in which the column is emptied and then immediately refilled with nitrogen, as we can see from the graph in just a couple of minutes.Considerazioni fluidodinamiche: Given:

- Column height = 1 meter = 100 cm
- Emptying time = 0.038 hours =136.8 s
- Emptying velocity = 100 (cm) / 136.8 (s) = 0,731 cm/s

Understanding the emptying velocity provides further insights into the fluid dynamics within the column.

1. **Flow Regime**

$$Re = \frac{\rho v D}{\mu} = 25.97$$

Where:

- ρ is the density of the gas (assumed to be nitrogen, ρ ≈ 1.25 kg/m3)
- v is the velocity (0.00731 m/s),
- D is the diameter of the column (0.05 m),
- μ is the dynamic viscosity of nitrogen (μ ≈ 1.76×10^{-5} Pa·s)

Since Re < 2000, the flow is laminar.

2. Pressure drop

The pressure drop for laminar flow can be calculated using the Poiseuille equation.

$$\Delta p = \frac{128 \mu L Q}{\pi D^4} = 0.0105\ Pa$$

Where Q is the volumetric flow rate.

The next step is to see what happens if we insert only inert material into the column: given the composition of the latter, we want to control the emptying time and whether it is possible to also use it as an adsorbent bed, as the cost would be decidedly lower. This is because there is a possibility that the inert material of which it is composed, i.e. 80% and 20% alumina, could react with the H2S in the absence of water. The latter is actually a rather remote possibility, as we have not been able to find evidence or academic articles about it.It is an efficient inorganic adsorbent, most of all due to its physical and chemical properties and low toxicity: many applications are reported in the literature, mainly involving reactions at high temperatures, like in our case. H2S has a pH value of circa 5, meaning it is acidic, and, according to the article, at this level there is a significantly strong electrostatic attraction between the positively charged surface of the adsorbents and the anionic ions resulting in the strong

adsorption capacity. For higher values, in fact, hydroxyl groups on the surface of the adsorbent becomes more negative in alkaline condition, due to the electrostatic repulsion between the adsorbent and adsorbate molecules.

The DURANIT 500X inert material used so far has been found to react with nitrogen, leading to the adsorption of H2S and HCl (include formulas), effectively reducing their concentrations within one hour. This phenomenon appears to be caused by the presence of 20% by weight of alpha-alumina. Calculations have shown a non-negligible adsorption capacity of approximately 10 µmol/g. According to academic literature, this value is consistent with that of an adsorbent material, prompting the need to replace the inert material.

A test was conducted with the column filled exclusively with pure alpha-alumina. Adsorption was again observed, with H2S being reduced after approximately three hours.

The next attempt will involve using glass spheres as the inert material.

The following section illustrates the MATLAB code used to evaluate the process dynamics, including adsorption capacity and the volume of H2S adsorbed. These calculations have been applied (so far) to three different cases, with further fluid dynamic considerations included.

```
clear all
close all
clc

% selezionare il file
[file, path] = uigetfile('dal27maggio.xlsx', 'Seleziona il file Excel');

if isequal(file, 0)
    disp('Nessun file selezionato');
else
    % percorso al file
    filename = fullfile(path, file);
    % leggi i dati dal file
    data = readtable(filename);

    % prendere solo ogni quinta riga
    data = data(1:5:end, :);

    % converti colonna data e ora in vettore datetime
    timestamps = datetime(data{:,1}, 'InputFormat', 'dd.MM.yyyy HH:mm:ss');
    % estrarre i valori di concentrazione di H2S
    h2s_concentration = data{:,2};
    % estrarre lo stato del processo
    process_state = data{:,3};

    % inizializza vettore concentrazione da manipolare
    modified_concentration = h2s_concentration;

    % soglia scostamento
    deviation_threshold = 1;

    % modifica i valori di concentrazione per 'analisi/pausa analisi'
    i = 1;
    while i <= length(process_state)
        if strcmp(process_state{i}, 'Analisi H2S') || strcmp(process_state{i}, 'Pausa
Analisi')
```

```
            % Identificare l'inizio e la fine del blocco
            start_idx = i;
            while i <= length(process_state) && (strcmp(process_state{i}, 'Analisi
H2S') || strcmp(process_state{i}, 'Pausa Analisi'))
                i = i+1;
            end
            end_idx = i-1;

            prev_value = NaN;
            next_value = NaN;

            % Trova il valore precedente in stato 'Lavaggio'
            for j = start_idx-1:-1:1
                if strcmp(process_state{j}, 'Lavaggio')
                    prev_value = h2s_concentration(j);
                    break;
                end
            end

            % Trova il valore successivo in stato 'Lavaggio'
            for j = end_idx+1:length(process_state)
                if strcmp(process_state{j}, 'Lavaggio')
                    next_value = h2s_concentration(j);
                    break;
                end
            end

            % media se entrambi i valori trovati
            if ~isnan(prev_value) && ~isnan(next_value)
                mean_value = (prev_value + next_value) / 2;
                modified_concentration(start_idx:end_idx) = mean_value;
            end
        else
            i = i + 1;
        end
    end

    % filtrare i dati per escludere le righe 'Fermo'
    valid_indices = ~strcmp(process_state, 'Fermo');
    valid_timestamps = timestamps(valid_indices);
    valid_concentration = modified_concentration(valid_indices);
    valid_states = process_state(valid_indices);

    % Sostituzione dei valori che si discostano troppo con la media dei valori
adiacenti
    for i = 2:length(valid_concentration)-1
        if abs(valid_concentration(i) - valid_concentration(i-1)) > deviation_threshold
&& abs(valid_concentration(i) - valid_concentration(i+1)) > deviation_threshold
            valid_concentration(i) = (valid_concentration(i-1) +
valid_concentration(i+1)) / 2;
        end
    end

    vol_flowrate = valid_concentration * 1.55 / 1e6; % Nm3/h

    time_diff = hours(valid_timestamps - valid_timestamps(1));
    MW = 34.1; % g/mol
    mass_flow = vol_flowrate * MW / 22.4; % kg/h
    molar_flow = 1000 * mass_flow / MW; % mol/h
    adsorbed_H2S = trapz(time_diff, vol_flowrate); % Nm3
    moli_H2S = trapz(time_diff, molar_flow); % mol
```

```
    m_alumina = 0.662;

    ads_capacity_al = moli_H2S / m_alumina; % mmol/g_al

    cumulative_hours = hours(valid_timestamps - valid_timestamps(1));

    % plot dati filtrati
    figure
    hold on

    % colori
    colors = containers.Map({'Analisi H2S', 'Lavaggio', 'Pausa Analisi'}, {'m', 'b',
'g'});
    legend_entries = {};
    legend_handles = [];

    % plot data
    for i = 1:length(valid_timestamps)-1
        state = valid_states{i};
        if colors.isKey(state)
            h = plot(cumulative_hours(i:i+1), valid_concentration(i:i+1), 'LineWidth',
1, 'Color', colors(state));
            if ~ismember(state, legend_entries)
                legend_entries{end+1} = state; %#ok<SAGROW>
                legend_handles = [legend_handles, h]; %#ok<AGROW>
            end
        end
    end

    % Scambia i nomi delle fasi 'Lavaggio' e 'Analisi H2S' nella legenda e traduci in
inglese
    for i = 1:length(legend_entries)
        if strcmp(legend_entries{i}, 'Lavaggio')
            legend_entries{i} = 'H2S Analysis';
        elseif strcmp(legend_entries{i}, 'Analisi H2S')
            legend_entries{i} = 'Washing';
        elseif strcmp(legend_entries{i}, 'Pausa Analisi')
            legend_entries{i} = 'Analysis Pause';
        end
    end

    xlabel('Cumulative hours (h)');
    ylabel('H2S (ppm)');
    grid on;
    box on;
    legend(legend_handles, legend_entries, 'Location', 'best');
    hold off
end
```

Table 8. Sorption test matrix

				Composition %.vol				
# TEST*	Components	T (°C)	V (Nm3/h)	N_2	H_2	CO_2	H_2O	H2S
1	N2	300	0,75	99,997%	0,00%	0,00%	0,00%	0,0030%
2	N2+CO2+H2	300	1	45,815%	29,87%	24,31%	0,00%	0,0050%
3	N2	300	1,25	16,380%	29,87%	24,31%	29,43%	0,0070%
4	Syngas	350	0,75	45,810%	29,87%	24,31%	0,00%	0,0070%
5	Syngas	350	1	16,387%	29,87%	24,31%	29,43%	0,0030%
6	N2+CO2+H2	350	1,25	99,995%	0,00%	0,00%	0,00%	0,0050%
7	Syngas	400	0,75	16,385%	29,87%	24,31%	29,43%	0,0050%
8	N2	400	1	99,990%	0,00%	0,00%	0,00%	0,0070%
9	N2+CO2+H2	400	1,25	45,817%	29,87%	24,31%	0,00%	0,0030%

The second MATLAB script below provided performs data processing and analysis on an H2S concentration dataset obtained from an Excel file downloaded from the datalog of the analyser.

The first column, which contains date and time information, is converted into a datetime vector using the datetime function with the specified input format ('dd.MM.yyyy HH:mm:ss'). The script extracts the H2S concentration values and the process state from the respective columns of the table.

Next, the script initializes a vector to hold the modified H2S concentration values and sets a deviation threshold of 1. It then iterates through the process_state vector to identify and modify the concentration values during 'Analisi H2S' and 'Pausa Analisi' states. For each block of these states, the script identifies the start and end indices and looks for the nearest 'Lavaggio' states before and after the block. If both values are found, the concentration values within the block are replaced with the average of these two values. This procedure is essential to ensure a more consistent and "smooth" data trend, thereby avoiding fluctuations caused by the conditioning phase ('Lavaggio'). During the 'Lavaggio' phase, the process conditions change, leading to potential variations in H2S concentration readings that do not reflect the actual process behavior. By averaging the concentration values before and after the 'Lavaggio' phase, the script mitigates these oscillations, resulting in a more accurate representation of the H2S concentration during 'Analisi H2S' and 'Pausa Analisi' phases. This refined data trend is crucial for subsequent analysis and interpretation, providing clearer insights into the process performance.

The script then filters the data to exclude rows where the process state is 'Fermo'. The remaining valid data is used to initialize vectors for the timestamps, concentration values, and process states. It also addresses any outliers in the concentration data by replacing values that deviate significantly from their adjacent values with the average of those adjacent values.

To calculate the volumetric flow rate, the script multiplies the valid concentration values by a factor (1.55 / 1e6) to convert the units to Nm3/h. The time differences are calculated in hours relative to the first timestamp. The script then calculates the mass flow rate using the

molecular weight of H2S (34.1 g/mol) and converts it to a molar flow rate. The total adsorbed H2S is determined by integrating the volumetric flow rate over time, yielding values in Nm3 and moles. To compute the adsorption capacity, the total moles of H2S are divided by the mass of alumina to obtain the adsorption capacity in mmol/g. The script also calculates cumulative hours for plotting purposes.

Finally, the script generates a plot of the valid H2S concentration data over time. It uses a color map to distinguish between different process states ('Analisi H2S', 'Lavaggio', 'Pausa Analisi'): the x-axis represents cumulative hours, and the y-axis represents H2S concentration in ppm.

6.2 Column with aggregate

While waiting for the glass beads to be delivered, a comprehensive test has been conducted with the testing conditions of test number 8 reported on Table 8. The reactor was filled as follows:

- Bottom: 50 mm Inert material (DURANIT X500)
- Middle: 40 mm Sorbent material Topsoe HTZ-5
- Top: 50 mm Inert material (DURANIT X500)

The graph in Figure 23 represents both the experimental result and the model result. A MATLAB model run with the same operative conditions, and a usage factor for the sorbent material equal to 30%. The first part of the graph may be emphasized by the effect of the inert material. This can be seen by a higher sorption efficiency compared to the standard model. Once the sorption capacity of the inert has been exhausted, the system's behaviour is similar to the model. Overall, the model can be considered a good representation of the experimental data. Unfortunately, a black-out occurred during the test after 25 hours from beginning. This caused the whole test procedure to be repeated and took 5 hours to stabilize the behaviour as before the accident.

Properties of the chosen aggregate (DURANIT-X 500):

Density of material	2,3 – 2,5 g/cm3
Free volume	40 - 45 %
Hardness (Mohs scale)	8
SiO2	≤ 80 %
Al2O3	≤ 20 %
TiO2	< 2 %
Fe2O3	< 1,5 %
CaO + MgO	≤ 1 %
K2O + NaO2	≤ 4 %

Based on the table, where I considered the average values for properties provided only as ranges, the following calculations were performed, assuming a 10 cm inert bed inside the column:

$$V_{column} = \frac{\pi}{4} D_{column}^2 h_{bed} = \frac{\pi}{4} (0{,}05\ m)^2 \cdot (0{,}1\ m) = 1{,}96 \cdot 10^{-4}\ m^3$$

$$V_{free} = 0{,}425 \cdot V_{column} = 8{,}44 \cdot 10^{-5}\ m^3$$
$$V_{inert} = V_{column} - V_{free} = 1{,}66 \cdot 10^{-4}\ m^3$$
$$m_{inert} = V_{inert} \cdot \rho_{inert} = (1{,}66 \cdot 10^{-4}\ m^3) \cdot (2400\ kg/m^3) = 0{,}268\ kg$$

Since we aim to determine the adsorption potential of alumina, based on the documentation available in various academic articles, we calculate its specific mass as follows:

$$m_{alumina} = 0{,}2 \cdot m_{inert} = 0{,}054\ kg$$

The same calculations and MATLAB code will be applied in the case of the column filled with pure alumina, with the difference that in this case, the mass will be equal to that of the inert material, as alumina is the only compound present.

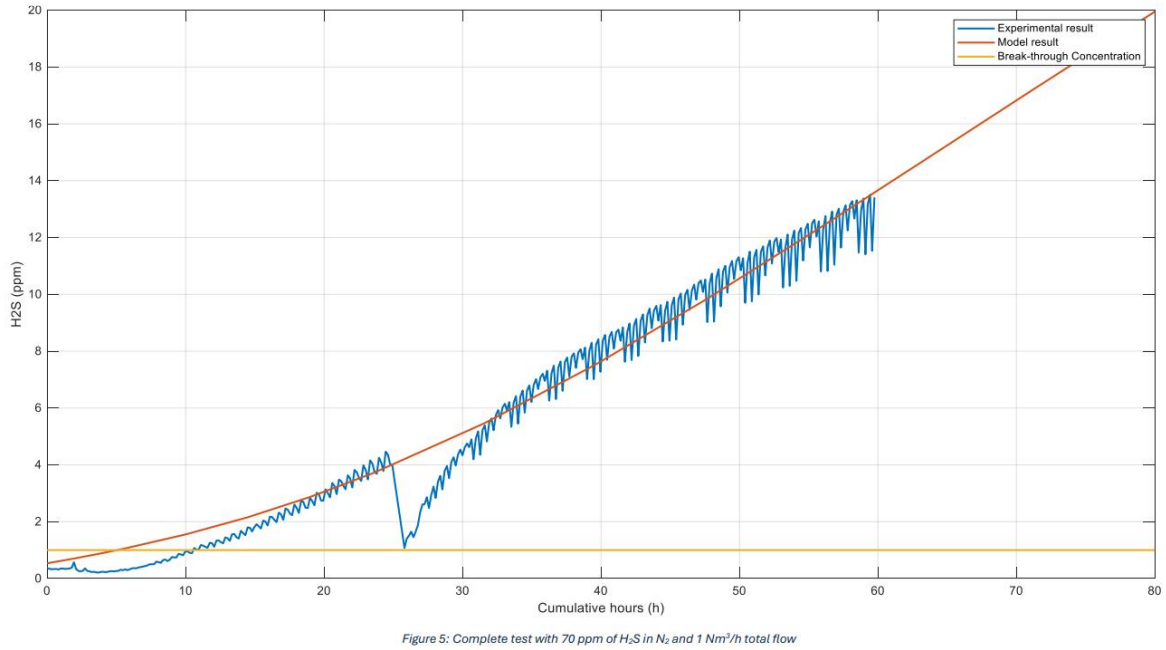

Figure 5: Complete test with 70 ppm of H_2S in N_2 and 1 Nm^3/h total flow

Figure 23. Complete test with 70 ppm of H2S and N2 and 1 Nm3/h total flow

$$Capacità\ di\ Adsorbimento = 5{,}74\ {\mu mol_{H2S}}/{g_{Al}}$$
$$Volume_{H2S\ adsorbiti} = 69\ Ndm^3$$

The plot also highlights the sequence phases: the initial phase, marked by the first peak, corresponds to the "Check composition" phase. Once 70 ppm is reached, the "Production" phase begins, where H2S is reduced in less than an hour.

6.3 Column filled with pure allumina

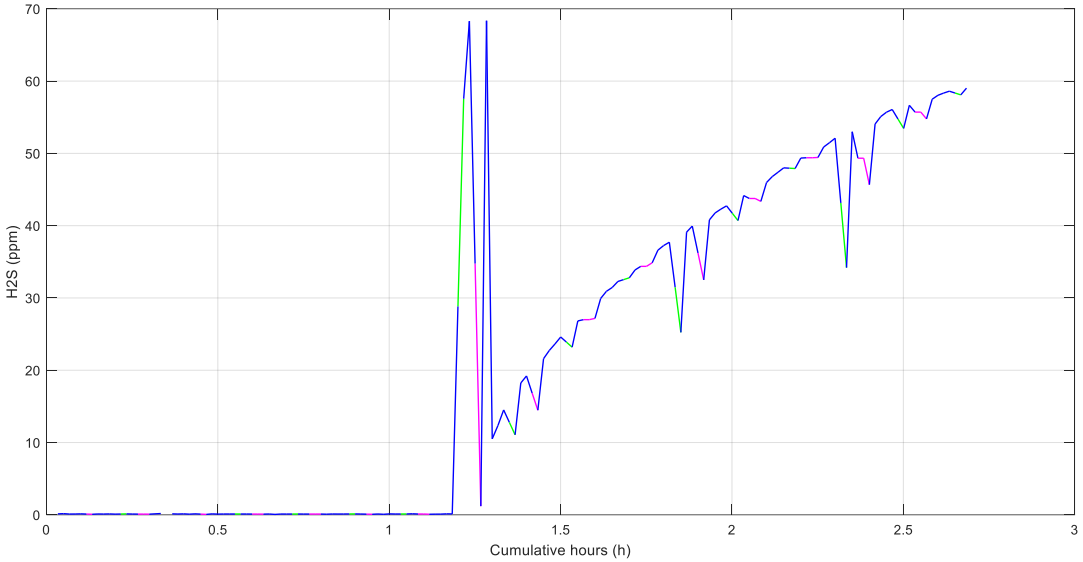

Figure 24. Test with pure allumina

$$V_{column} = \frac{\pi}{4} D_{column}^2 h_{bed} = \frac{\pi}{4} (0{,}05\ m)^2 \cdot (0{,}1\ m) = 1{,}96 \cdot 10^{-4}\ m^3$$

$$V_{free} = 0{,}425 \cdot V_{column} = 8{,}44 \cdot 10^{-5}\ m^3$$
$$V_{inert} = V_{column} - V_{free} = 1{,}66 \cdot 10^{-4}\ m^3$$
$$m_{inert} = V_{inert} \cdot \rho_{inert} = (1{,}66 \cdot 10^{-4}\ m^3) \cdot (3990\ \ kg/m^3) = 0{,}662\ kg$$

Results:

$$Capacità\ di\ Adsorbimento = 3{,}4\ {}^{\mu mol_{H2S}}/_{g_{Al}}$$
$$Volume_{H2S\ adsorbiti} = 50{,}8\ Ncm^3$$

6.4 Hydrogen interference test

The H2S analyser is based on an electrochemical cell sensor technology. Hydrogen interferes on the measurement as the electrochemical sensors is sensitive to this compound as well. The aim of the tests was to quantify the interference of H2 on the H2S measurement. The tests consisted in feeding the analyser with three different mixtures of H2 in N2 to the analyser and logging the measured values. The results are reported in Figure 2. It can be observed as adding hydrogen has an important effect on the measurement that needs to be taken into account compensated for during the tests where H2 is present.

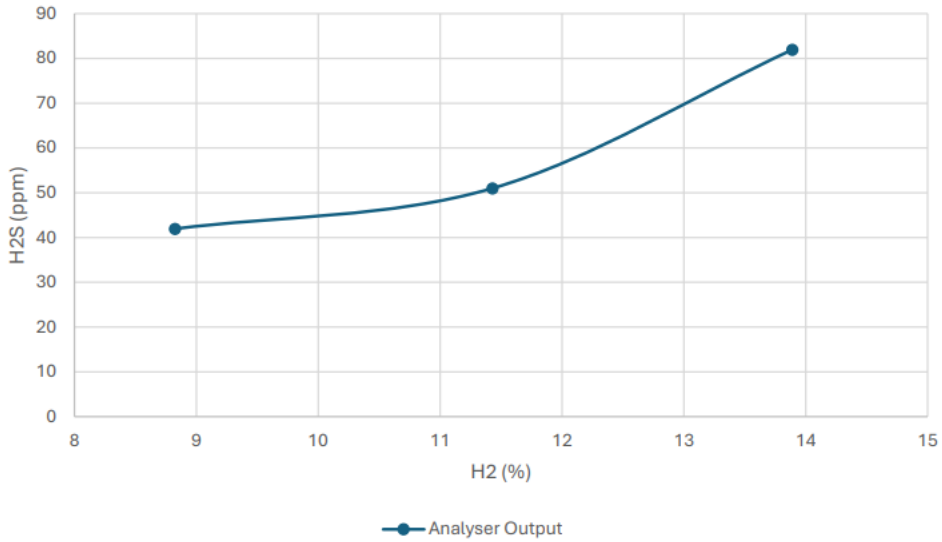

Figure 25. Hydrogen effect on H2S sensor

The effectiveness of an adsorption process heavily depends on the selection of a suitable adsorbent. Several factors to consider when choosing an adsorbent or an adsorption process are outlined as follows:

1. Ease of separation: if the mixture components have similar volatilities, using a distillation column might be too costly in terms of both capital and operational expenses. In such cases, adsorption can be a more practical option.

2. Solute concentration: adsorption is advantageous when the target component's concentration is low. For instance, if an aqueous organic compound is present in low concentration, distillation would require vaporizing the entire mixture, which consumes a lot of energy. Adsorption offers a more energy-efficient and straightforward solution, particularly in treating various waste streams, including gaseous ones containing organic compounds.

3. Process conditions: adsorption is often preferred when mild processing conditions are necessary, especially when a product could degrade or get damaged by more intense conditions.

4. Adsorbent characteristics: a good adsorbent should have several key properties, including high adsorption capacity, ability to reverse the adsorption process, selectivity, ease of regeneration, low cost, insolubility, and good mechanical strength (when used in bead or pellet form). Among these, adsorption capacity is typically the most critical, as it reflects how much solute can be adsorbed per unit mass of the adsorbent.

The objective of the hydrogen interference tests is to quantify how the presence of H2 affects the H2S readings on an analyzer based on electrochemical sensor technology. The electrochemical sensors used in H2S analyzers are also sensitive to hydrogen, leading to potential interference in the measurement: in order to accurately compensate for this interference, the tests aim to determine the extent of the effect of H2 on the H2S readings. The

tests involve feeding the analyzer with three different mixtures of H2 in N2 and logging the measured values. From the figure, it can be observed that the addition of hydrogen has a significant effect on the measurement, which needs to be taken into account and compensated for during tests where H2 is present.

In order to carry out a test with the addition of hydrogen, it is first necessary to make some preliminary calculations to determine the variation in flow rates and the consequent dilution of H2S. It is necessary to balance the incoming and outgoing gases with the final concentration as the unknown, keeping the flow rates of N2 and N2 with H2S constant.

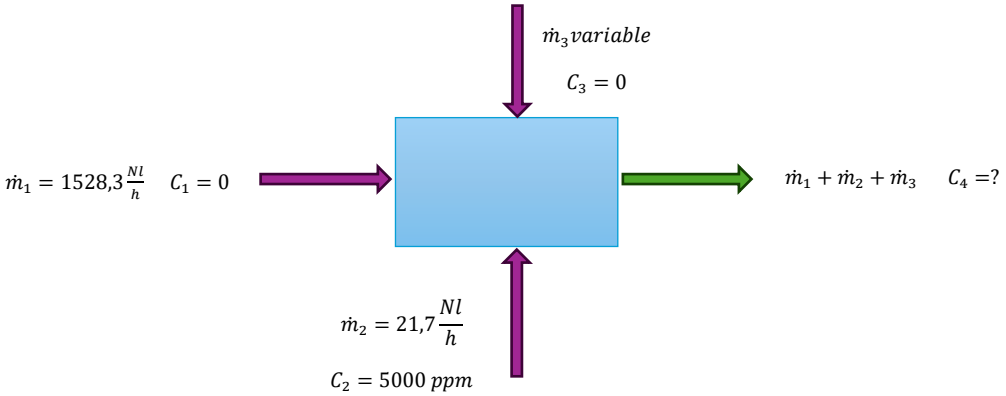

$$\dot{m}_1 C_1 + \dot{m}_2 C_2 + \dot{m}_3 C_3 = (\dot{m}_1 + \dot{m}_2 + \dot{m}_3) C_4$$

Thus,

$$C_4 = \frac{\dot{m}_2}{\dot{m}_1 + \dot{m}_2 + \dot{m}_3} C_2$$

N2 (Nl/h)	H2S + N2 (Nl/h)	H2 (Nl/h)	N2 + H2S + H2 (Nl/h)	C2 (ppm)	C4 (ppm)	
1528.3	21.7	10	1560	5000	69.55128205	0.0000696
1528.3	21.7	20	1570	5000	69.10828025	0.0000691
1528.3	21.7	30	1580	5000	68.67088608	0.0000687
1528.3	21.7	40	1590	5000	68.23899371	0.0000682
1528.3	21.7	50	1600	5000	67.8125	0.0000678
1528.3	21.7	100	1650	5000	65.758	0.0000658
1528.3	21.7	150	1700	5000	63.824	0.0000638
1528.3	21.7	200	1750	5000	62	0.0000620
1528.3	21.7	250	1800	5000	60.278	0.0000603
1528.3	21.7	300	1850	5000	58.649	0.0000586

To calculate the percentages of each component, however, the following formulas were used:

$$\% N_2 = \frac{\dot{m}_1 + \dot{m}_2(1 - C_4)}{\dot{m}_1 + \dot{m}_2 + \dot{m}_3}$$

$$\% H_2S = \frac{\dot{m}_2 \cdot C_4}{\dot{m}_1 + \dot{m}_2 + \dot{m}_3}$$

Consequently, the percentage of hydrogen can also be obtained.

N2 (%)	H2S (%)	H2 (%)
99.358878	0.000097	0.641025641
98.726019	0.000096	1.27388535
98.101172	0.000094	1.898734177
97.484184	0.000093	2.51572327
96.874908	0.000092	3.125
93.939307	0.000086	6.060606061
91.176389	0.000081	8.823529412
88.571352	0.000077	11.42857143
86.111038	0.000073	13.88888889
83.783715	0.000069	16.21621622

Conclusion

The goal of my thesis was to evaluate and optimize the adsorption of acidic compounds, particularly hydrogen sulfide (H_2S), within the framework of the Micro-Bio-CHP project. The experimental tests conducted have demonstrated that H_2S can be effectively adsorbed within the expected timeframe, aligning with the project's target for the removal of harmful contaminants from the process stream. However, due to time constraints, we were unable to conduct tests involving CO_2 and water, which are essential for a more comprehensive validation of the adsorption system. These additional tests would provide further insights into the performance of the system under real-world conditions, where moisture and carbon dioxide are typically present. Furthermore, in order to enhance the system's efficiency even further, it would be beneficial to conduct tests with an inert material such as glass spheres. This would allow us to better understand the potential for optimizing the adsorbent's packing and flow dynamics.

Thus we can assert that while the work completed has brought us closer to the project's objectives, achieving satisfactory adsorption of H_2S within the projected timeframes, further testing and refinement are required to ensure optimal performance across a broader range of operating conditions: the results so far are promising and suggest that the system is on the right track, but there are additional steps needed to fully meet the ambitious goals of the project.

References

Li, M., Bo, X., Mu, Z., & Zhang, Y. (2013*). Reduced graphene oxide/multiwalled carbon nanotubes hybrid material for constructing a high-performance electrochemical sensor for nicotinamide adenine dinucleotide*. Applied Surface Science*, 282*, 718-723.

Udomsilp, S., et al. (2020). *Hydrogen sulfide removal from biogas using metal oxide adsorbents: A review.* Renewable and Sustainable Energy Reviews, 133, 110307.

Muñoz, R., Meier, L., Diaz, I., Jeison, D. (2015). *A review on the state-of-the-art of physical/chemical and biological technologies for biogas upgrading.* Renewable and Sustainable Energy Reviews, 40, 428-440.

D. Di Profio, *Progettazione e sviluppo di un banco sperimentale per la rimozione di acido cloridrico e solfidrico da product gas derivante dalla gassificazione di combustibili lignocellulosici,* Politecnico di Torino, 2023.

Jansen, D., Gazzani, M., Manzolini, G., et al. (2015). *Pre-combustion CO2 capture*. International Journal of Greenhouse Gas Control, 40, 167-187.

Müller, L., Wolff, S., van Leeuwen, C., & Giesen, A. (2017). *Biogas upgrading technologies: developments and innovations.* Energy Procedia, 114, 530-538.

Kim, Y., Lee, S., Kim, K., (2018*). Adsorption isotherm models and the heat of adsorption of CH4 and CO2 on activated carbon prepared from waste palm trunk.* Chemical Engineering Journal, 359, 48-57.

Deng, S., Bai, R., Chen, J. P. (2003*). A comparative study of the adsorption behavior of ammonium onto natural zeolites.* Water Research, 37(18), 4673-4682

Cheremisinoff, N. P. (2013*). Handbook of Solid Waste Management and Waste Minimization Technologies*. Butterworth-Heinemann.

Abatzoglou, N., & Boivin, S. (2009). *A review of biogas purification processes*. Biofuels, Bioproducts and Biorefining, 3(1), 42-71.

Kaltschmitt, M., Thrän, D. (2018). *Renewable Energy from Biomass.* Springer Handbook of Bio-/Cogeneration Systems. Springer, Berlin, Heidelberg.

European Biogas Association. (2023). *Biogas and Biomethane Report 2023.* Disponibile su: https://www.europeanbiogas.eu/

Horizon 2020. *Micro-Bio-CHP Project Description.* Disponibile su: https://cordis.europa.eu/project/id/731187

HYSYTECH S.r.l. (2024). *Innovative energy solutions for industrial applications.* Disponibile su: https://www.hysytech.com

European Commission. *Directive 2012/27/EU on energy efficiency*. Disponibile su: https://eur-lex.europa.eu

Aspen Plus. (2024). *Aspen Plus Simulation Software Documentation*. Aspen Technology, Inc.

MATLAB. *Optimization Toolbox: User's Guide*